HUMAN RETINAL PIGMENT EPITHELIAL LYSIS OF EXTRACELLULAR MATRIX: FUNCTIONAL UROKINASE PLASMINOGEN ACTIVATOR RECEPTOR, COLLAGENASE, AND ELASTASE

BY *Susan G. Elner, MD*

ABSTRACT

Purpose: To show (1) human retinal pigment epithelial (HRPE) expression of functional urokinase plasminogen activator receptor (uPAR; CD87), (2) HRPE secretion of collagenase and elastase, (3) uPAR-dependent HRPE migration, and (4) uPAR expression in diseased human retinal tissue.

Methods: Immunohistochemistry for uPAR was performed on cultured HRPE cells and in sections of human retina. Double-immunofluorescent staining of live human RPE cells with anti-CR3 antibody (CD11b) was performed to demonstrate the physical proximity of this ß2 integrin with uPAR and determine whether associations were dependent on RPE confluence and polarity. Extracellular proteolysis by HRPE uPAR was evaluated using fluorescent bodipy-BSA and assessed for specificity by plasminogen activator inhibitor-1 (PAI-1) inhibition. The effect of interleukin-1ß (IL-1ß) on uPAR expression was assessed. Collagenase and elastase secretion by unstimulated and IL-1–stimulated HRPE cells was measured by ^{3}H-labelled collagen and elastin cleavage. HRPE-associated collagenase was also assessed by cleavage of fluorescent DQ-collagen and inhibited by phenanthroline. Using an extracellular matrix assay, the roles of uPAR and collagenase in HRPE migration were assessed.

Results: Immunoreactive uPAR was detected on cultured HRPE cells and increased by IL-1. On elongated, live HRPE cells, uPAR dissociated from CD11b (CR3) and translocated to anterior poles of migrating cells. Extracellular proteolysis was concentrated at sites of uPAR expression and specifically inhibited by PAI-1. Cultured HRPE cells secreted substantial, functional collagenase and elastase. IL-1 upregulated uPAR, collagenase, and elastase activities. Specific inhibition of uPAR, and to a lesser degree collagenase, reduced HRPE migration in matrix/gel assays. Immunoreactive uPAR was present along the HRPE basolateral membrane in retinal sections and in sections of diseased retinal tissue.

Conclusions: HRPE cells express functional uPAR, collagenase, and elastase, which may permit HRPE proteolysis and migration. uPAR polarization may concentrate proteolysis at the leading edge of migrating HRPE cells.

Trans Am Ophthalmol Soc 2002;100:273-299

INTRODUCTION

Disruption of collagen- and elastin-rich Bruch's membrane that underlies the retinal pigment epithelium (RPE) and periretinal RPE cellular migration occur in several important retinal diseases, including age-related macular degeneration (ARMD) and proliferative vitreoretinopathy (PVR). Urokinase plasminogen activator receptor (uPAR CD87) and matrix metalloproteinases (MMPs) are important mechanisms by which leukocytes, vascular endothelial cells, reactive tissue cells, and neoplastic cells penetrate extracellular matrix (ECM) in virtually all tissues. However, uPAR, by activating plasminogen to form plasmin, yields proteolytic activity that lyses a wide variety of ECM components when compared to the MMP.

These observations lead to the hypothesis that RPE uPAR-mediated activation of proteolysis, in contrast to secretion of enzymes cleaving elastin, interstitial collagen, and type IV collagen, mediates RPE migration through ECM and is expressed in retinal lesions.

This study demonstrates the following for the first time: (1) RPE uPAR expression in situ; (2) proinflammatory cytokine–enhanced immunoreactive and functional RPE uPAR activity; (3) RPE secretion of interstitial collagenase and elastase capable of hydrolyzing natural substrates; (4) the preeminent role of RPE uPAR in mediating RPE migration through extracellular matrix using a novel three-dimensional collagen gel assay technique; and (5) RPE uPAR expression in human lesions of subretinal choroidal neovascularization associated with Bruch's membrane disruption, proliferative vitreoretinopathy with

From the University of Michigan and University of Chicago. This work was supported by grants EY-09441 and EY-007003 from the National Institutes of Health.

RPE periretinal migration into the matrix of periretinal membranes, and uveitis with chronic active inflammation. In so doing, this study indicates that uPAR is important to RPE participation in retinal pathology.

BACKGROUND

Age-related macular degeneration is the most common cause of legal blindness in patients over the age of 50 from developed countries.[1] The early manifestations of ARMD involve Bruch's membrane thickening and formation of extracellular matrix- and lipid-containing deposits.[1] Focal collections of this material enlarge to form drusen, which is the hallmark finding in ARMD.[2] The mechanism by which this material is deposited in Bruch's membrane is not well understood, but it is commonly believed to be derived from the aged or dysfunctional RPE cells.[2,3,4] Accompanying the changes in Bruch's membrane are progressive degradative changes in the RPE with pigmentary and atrophic alterations in RPE that become clinically apparent. Although most patients with ARMD exhibit the atrophic form, composed of drusen and RPE alterations, severe vision loss usually results from choroidal neovascularization (CNV), which complicates ARMD. ARMD neovascularization originates from the vessels in the choriocapillaris of the choroid and grows through breaks in the altered, thickened Bruch's membrane, to extend either beneath the RPE or the sensory retina. The RPE has been noted to be a major component of CNV both in postmortem[5-7] and in surgical CNV specimens. RPE cells migrate from their normal position on Bruch's membrane and grow over the surface of the CNV as it penetrates through Bruch's membrane.[8-12]

Although a genetic component in typical ARMD is suggested by a familial tendency in some patients, a specific genetic defect has not been identified. Sorsby's fundus dystrophy is an autosomal dominant macular disorder, less common than ARMD, that strikes patients at an earlier age. It shares most of the clinical and pathophysiologic features of ARMD. In Sorsby's dystrophy, like ARMD, atrophy of the RPE, choriocapillaris, and photoreceptors may occur, with frequent development of CNV, resulting in severe visual loss. Sorsby's has been mapped to human chromosome 22, the same region to which the tissue inhibitor of matrix metalloproteinase-3 (TIMP-3) gene has been mapped.[13] Tissue inhibitor of matrix metalloproteinases regulate MMPs, which are a family of enzymes whose chief function is the degradation of ECM, including ECM components found in Bruch's membrane.[14] Point mutations in the TIMP-3 gene, which render the altered TIMP-3 defective, have been identified in affected members of Sorsby's fundus dystrophy families, implicating it in the pathogenesis of this dystrophy.[15] TIMP-3 is unique among TIMPs because upon secretion, it binds to extracellular matrix components. Thickening of Bruch's membrane is a hallmark of Sorsby's dystrophy.[16] Studies have demonstrated increases in TIMP-3 in Bruch's membrane in Sorsby's patients, except in areas in which RPE cells have degenerated.[17] An accumulation of TIMP-3 in the ECM of Bruch's membrane may result in excessive ECM remodeling and lead to abnormal Bruch's membrane thickening noted in Sorsby's dystrophy and ARMD.[15,18] The reactive alterations in Bruch's membrane predispose to the development of breaks in this tissue through which ingrowth of new vessels from the choriocapillaris may occur.[19-23] However, the process of how breaks develop in Bruch's membrane remains unknown.

THE MATRIX METALLOPROTEINASES

The MMPs are a family of enzymes that hydrolyze protein components of the ECM and are involved in normal ECM turnover, remodeling, and connective tissue turnover.[24] In addition, they have been found to play important roles in many normal and pathologic processes, such as angiogenesis,[25,26] wound healing,[24] ovulation,[27] trophoblast invasion,[28] skeletal development,[29,30] arthritis,[31,32] cancer invasion and metastasis,[33,34] aneurysmal formation,[35] and atherosclerotic plaque rupture.[36-38]

MMPs have been categorized into more than 20 groups on the basis of their substrate specificity.[39] They are also known by their common group names, interstitial collagenases (MMP 1,8,13), gelatinases (MMP 2,9), stromelysins (MMP 3,10,11), and membrane-type MMPs (MT-MMP 14-17, 24,25) (Table I). MMPs are secreted as inactive proenzymes that require activation by the removal of a propeptide, to reveal a zinc-active binding site. MMP activity may be regulated at a number of stages, including (1) gene activation and transcription, (2) translation, (3) secretion of the latent proenzyme, (4) proenzyme activation, and (5) inactivation by endogenous inhibitors (ie, TIMPs).

The interstitial collagenases are primarily responsible for the degradation of structural collagens types I, II, and III.[40] MMP-1, or collagenase 1, is the most ubiquitously expressed and is produced at low constitutive levels by fibroblasts, macrophages, and endothelial cells and at higher constitutive levels by many tumor cells.[41] Expression of MMP-1 is upregulated by inflammatory cytokines and growth factors.[41] MMP-1 expression has been associated with low survival rates in many tumors, including esophageal and pancreatic cancer.[42-44]

Gelatinases A and B primarily degrade collagen type IV but can degrade collagen types I, V, and gelatin.[27] They are believed to play a particularly important role in angiogenesis.[26] Gelatinase A, MMP-2, is regulated differently than all other MMPs, both transcriptionally and extracel-

TABLE I: NOMENCLATURE OF MATRIX METALLOPROTEINASES (MMPS)

CLASS	COMMON NAME	MMP	MAJOR SUBSTRATES
Collagenases	Collagenase 1	MMP1	Types I, II, III, VII collagens
	Collagenase 2	MMP8	
	Collagenase 3	MMP13	
Gelatinases	Gelatinase A	MMP2	Types I, IV, V collagens, gelatin
	Gelatinase B	MMP9	
Stromelysins	Stromelysin 1	MMP3	Fibronectin, laminin, collagens IX, X, elastin
	Stromelysin 3	MMP11	
Membrane-type MMPs	MT1-MMP	MMP14	Activate latent gelatinase A
	MT2-MMP	MMP15	
	MT3-MMP	MMP16	

lularly.[45] The promotor of the gelatinase A gene lacks the TPA (12-tetradecanoylphorbol-13-acetate) responsive element and the transactivator sequences, AP-1 and PEA-3.[46] The promotor also lacks a transforming growth factor-beta (TGF-ß) inhibitory element. As a result, gelatinase A is not upregulated by phorbol myristate acetate (PMA), tumor necrosis factor alpha (TNF-α), interleukin-1 (IL-1), plasmin, or trypsin, nor is it inhibited by TGF-ß.[30] The gelatinases are inactivated either by TIMPs, which bind to their catalytic domain, or by autocatalysis, mechanisms that prevent uncontrolled proteolysis.[47,48]

Latent, pro–gelatinase A is constitutively secreted by vascular and synovial endothelial cells, monocytes, lymphocytes, dendritic cells, fibroblasts, and tumor cells,[49, 50] whereas other MMPs are not constitutively expressed. Unlike other MMPs, gelatinase A can be activated on cell surfaces via two mechanisms: (1) MT1-MMP and type I collagen, and (2) thrombin and serine protease, activated protein C.[26,30] When activated by the MT1-MMP pathway, TIMP-2 binds to MT1-MMP on the cell surface; pro–gelatinase A then binds to TIMP-2 and is cleaved to its active form by an adjacent MT1-MMP on the cell surface. Collagen I promotes gelatinase A activation by upregulating MT1-MMP. Activation via the activated protein C–thrombin pathway occurs more rapidly than activation via collagen I and is independent of MT1-MMP. Thrombin binds thrombomodulin on the endothelial cell surface, which leads to the conversion of protein C to activated protein C. Activated protein C, in turn, rapidly activates gelatinase A, occurring even in the absence of cells.[26] The thrombin–activated protein C activation pathway for gelatinase A may be particularly important in the angiogenesis of cancer and rheumatoid arthritis, since high levels of thrombin are present in these conditions.[51]

Gelatinase B, MMP-9, is not constitutively expressed, but is produced by a variety of cells, including epithelial cells, fibroblasts, endothelial cells, neutrophils, monocytes, and lymphocytes in response to many stimuli, including lipopolysaccharide (LPS), viruses, cytokines, and cell-cell contact.[34,50] Gelatinase B is stored in both active and latent forms in the cell cytosol in secretory vesicles.[52] Release of gelatinase B from neutrophil granules occurs rapidly in response to interleukin-8 (IL-8). Secreted gelatinase B is bound to TIMP-1, while cytosolic gelatinase B is not bound to TIMP-1.[26] Because of the difference in constitutive expression between gelatinases A and B, the ratio of gelatinase B over gelatinase A has been used as a marker of inflammation in autoimmune diseases such as rheumatoid arthritis and multiple sclerosis.[53,54]

The gelatinases function as regulators of cytokines and chemokines. Gelatinase B promotes inflammation by converting the proform of IL-1ß into the active cytokine.[55] It also cleaves IL-8, a major chemoattractant for neutrophils, into a more active form, potentiating IL-8 effects. Neutrophils attracted and stimulated by IL-8 may then release more gelatinase B, potentiating the inflammatory response.[50] Gelatinases also antagonize chemokine activity. Gelatinase A cleaves monocyte chemotactic protein-3 (MCP-3), a chemoattractant for monocytes, into a less active form, thereby dampening the leukocytic infiltration.[56]

MMP-3 or stromelysin-1 can degrade a variety of ECM proteins, including fibronectin, laminin, elastin, and collagens IX and X.[57] Stromelysins also indirectly contribute to the collagen degradation by their activation of other latent MMPs.[40] MMP-3 is expressed in atherosclerotic lesions, particularly in areas of the plaque where rupture is most common, implicating MMPs in ECM resorption that may result in plaque instability and rupture.[37, 38] There has also been evidence to suggest that MMP-3 may contribute to the development of aneurysms.[58]

MT-MMPs are membrane-bound MMPs that cleave

collagen fibrils into classic 1:3 fragments and serve to activate other latent MMPs, particularly gelatinase A. MT-MMPs are synthesized in a latent form but are activated intracellularly, by a furin-dependent mechanism. MT-MMPs have been implicated in tumor invasion, with increased levels of MT1-MMP found in normal stromal cells adjacent to tumors.[41]

MATRIX METALLOPROTEINASES IN THE RETINA

A number of MMPs have been noted in ocular tissues, most being associated with the RPE. Cultured human RPE cells have been shown to secrete basal levels of latent interstitial collagenase (MMP-1), stromelysin (MMP-3), gelatinases A (MMP-2) and B (MMP-9), and TIMP-1.[59] These MMPs have shown variable expression to stimulants. The phorbol ester, TPA, increases MMP-1, -2, -3, and -9, whereas TPA decreases TIMP-1.[59, 60] The proinflammatory cytokine, IL-1, stimulates production of MMP-1 and MMP-9, but the anti-inflammatory, fibrogenic cytokine, TGF-ß, does not.[61] Immunohistochemical studies of sections from post-mortem human eyes have identified MMP-2 and MT1-MMP in situ in the RPE, retina, and choroid.[62] Studies have demonstrated TIMP-3, which has been associated with Sorsby's macular degeneration, in the RPE, implicating the RPE as a likely source of TIMP-3 found in the thickened abnormal Bruch's membrane.[63] MMPs of all classes have been identified in the RPE, thereby giving the RPE the capability of modulating ECM remodeling and degradation in their surrounding milieau.

UROKINASE PLASMINOGEN ACTIVATOR AND ITS RECEPTOR uPAR

Another well-known modulator of extracellular matrix is the serine protease, urokinase plasminogen activator (uPA), which catalyzes conversion of inactive plasminogen to its active form, plasmin.[64] Plasmin is a broad-spectrum protease that degrades fibrin and most substrates in the ECM, including fibronectin and laminin. uPA is secreted by a wide variety of cells in tissues, including those of the retina and choroid, as a single-chain polypeptide (pro-uPA), which is enzymatically inactive. Pro-uPA binds with high affinity to its receptor, urokinase plasminogen activator receptor (uPAR; CD87), a single-chain 55 to 60 kD glycoprotein that is anchored to cell membranes by a glucosylphosphatidylinositol (GPI) moiety.[65] uPAR binds the amino-terminal domain of pro-uPA, leaving the catalytic, carboxyl terminal domain open.[66] Pro-uPA is enzymatically cleaved in its uPAR-bound form into a two-chain active enzyme by plasmin. uPA then, in turn, converts membrane-associated plasminogen into plasmin.[64] uPAR has been identified on activated monocytes,[66] T-lymphocytes,[67] neutrophils,[68] a variety of nonhematopoietic cells (including endothelial cells, fibroblasts, hepatocytes, keratinocytes),[69,70,67] and many tumor cells (including melanoma, breast, colon, prostate carcinoma).[67,71,72]

Activity of uPA and its receptor, uPAR, is correlated with ECM proteolysis, alterations in cell adhesion, cell motility, and cellular invasion through the ECM.[73] uPA or receptor-bound uPA can be blocked by two endogenous inhibitors known as plasminogen activator inhibitor 1 and 2 (PAI-1 and PAI-2),[64] which belong to the serpin protease superfamily. Several growth factors and cytokines have been implicated in uPA/uPAR regulation, including epidermal growth factor (EGF),[74] basic fibroblast growth factor (bFGF),[75] TGF-α,[76] and TNF-α.[77]

uPAR functions to (1) bind uPA, mediate the internalization of uPA/PAI complexes, and direct uPA proteolytic activity[78,79]; (2) stimulate cell proliferation when bound to uPA[80]; (3) induce chemotactic cell migration of leukocytes and multiple other cell types through activation of uPA; (4) promote cell-cell and cell-ECM adhesion via binding to vitronectin or through interactions with $ß_1$ or $ß_2$ integrins; (5) mediate signal transduction; (6) promote differentiation in myelomonocytic cells; and (7) activate monocytes and T-lymphocytes.[81,82] Through these cellular functions, uPA/uPAR has been shown to play an important role in proteolysis, cell migration, angiogenesis, leukocyte chemotaxis, and tumor invasion and metastasis.

uPA/uPAR IN THE RETINA

Studies of uPA/uPAR in the eyes have been limited to immunohistochemical localization. These studies have shown that uPA appears to have a wide tissue distribution in the posterior segment of the eye, where it is located in the optic nerve, sclera, choroidal fibroblasts, blood vessels, vitreous, inner neural retina, and RPE.[83] Moreover, RPE cells in vitro have been shown to produce immunoreactive uPA[84] and a possible inhibitor, PAI, which is immunologically and biochemically similar to PAI-1.[84,85] Studies had reported indirect stimulation of uPA activity in RPE cells in response to interferon-gamma (IFN-γ) by suppression of PAI expression.[86] Limited studies have been performed on the expression of uPAR and its regulation in RPE cells. Thrombin[87] and TGF-ß[88] have been shown to induce uPAR mRNA, resulting in an increase of uPAR on the RPE cell surface. In contrast, IFN-γ, despite increasing uPAR mRNA, was not reported to increase RPE cell-surface uPAR.[88] These studies, however, have not demonstrated RPE uPAR function and its modulation by proinflammatory cytokines, interactions with other RPE cell surface ligands, alterations of distribution with changes in RPE morphology, or its presence in diseased retinal tissues.

REGULATION OF CELL MIGRATION IN PVR

The presence of MMPs and uPAR is not only important in

the pathogenesis of ocular diseases, which involve ECM degradation, but these enzymes also may play roles in diseases that involve cell migration, such as PVR and uveitis. In PVR, RPE cells migrate from their position on Bruch's membrane, where their attachment is in part formed by $ß_1$ integrin binding to fibronectin, laminin, and collagen IV lining the vitreous and retinal surfaces. RPE migration and proliferation at these sites contribute to periretinal and vitreous membrane formation. PVR membranes have been shown to be composed of collagen types I, II, III, and, to a lesser degree, laminin and collagen types IV and V.[89] During PVR, the RPE cells have been noted to produce new ECM around themselves, which contains molecules similar to their original basement membrane firmly anchoring the RPE cells in these pathologic membranes.[90] MMPs may be important in the remodeling of ECM, which occurs during PVR. A number of cytokines, including IL-1, TNF-α, IFN-γ, IL-6, MCP-1, and macrophage colony-stimulating factor (M-CSF), have been noted in PVR[91-93] and may, in part, direct migration, proliferation, and transformation of RPE cells.[94]

Cellular migration, however, can be affected by interactions between uPA/uPAR, integrins, and MMPs. uPA/uPAR promotes cell migration by (1) degradation of ECM proteins, allowing cells to cross basement membranes,[95] both directly through its activation of plasminogen to plasmin and indirectly via the activation of proMMPs by uPA,[96] (2) direct chemotactic effects of both uPA and uPAR on capillary endothelial cells, keratinocytes, fibroblasts, and neutrophils,[97-99] (3) uPAR binding to vitronectin, an adhesive glycoprotein, promoting cell migration by inhibiting adhesion to fibronectin or fibrinogen,[100] and (4) uPAR colocalization with adhesion molecules, integrins, and cadherins, modulating cell adhesion and migration. In particular, uPAR physically associates with the leukocyte integrin CD11b/CD18 (CR3/Mac 1), which has been demonstrated on RPE cells.[101,102] The association of uPAR and CD11b changes depending on cell shape. In resting cells, uPAR and CD11b colocalize, but following cell polarization (elongation) and migration, the receptors dissociate, with CD11b concentrating in the uropodia and uPAR concentrating in the lamellipodia (leading edge).[103] In view that CD11b regulates cell adhesion, chemotaxis, and cell migration in many cell types, uPAR may further modulate migration.

The MMPs may also modulate cell migration via a number of methods, including (1) proteolysis of ECM, (2) cleavage and inactivation of proinflammatory cytokines, which may stimulate cell chemotaxis,[104] (3) MMP downregulation of uPAR-mediated proteolysis[105] via MMP-12 cleavage of the uPAR domain responsible for uPA binding, thereby limiting uPAR activity,[106] and (4) cleavage of adhesion molecules CD44 and L-selectin.[107,108]

Since RPE cells possess $ß_1$ integrins and uPA/uPAR and produce a variety of MMPs, all of which may effect migration and proteolysis, this study was undertaken to further elucidate the role of uPAR in RPE migration and proteolysis by (1) studying the modulation of uPAR by proinflammatory cytokines, (2) studying and comparing the effects of functional uPAR and interstitial collagenases on RPE migration and proteolysis, and (3) studying the expression of uPAR in diseased retinal tissues.

MATERIALS AND METHODS

HUMAN RPE CELL CULTURE AND ISOLATION

Human RPE cells were isolated from donor eyes as previously described[109] and cultured in Dulbecco's modified essential medium (DMEM) containing 15% fetal bovine serum. The cultured RPE cells formed monolayers showing typical polygonal morphology and pigmentation of scattered cells as well as the expression of cytokeratin.[110] Primary, first passaged, and second passaged RPE cell cultures were trypsinized and seeded onto either gel-coated slides for proteolysis studies, gelatin-nylon mesh matrix in 35-mm culture wells in the same media for migration studies, or glass coverslips for immunohistochemical staining. RPE cultures were maintained in the media and observed by phase contrast microscopy until they reached confluence. They were used in migration or proteolysis assays or processed for light microscopy and/or immunohistochemistry.

IMMUNOHISTOCHEMICAL STAINING FOR UROKINASE PLAMINOGEN ACTIVATOR RECEPTOR

Human RPE cell culture preparations on glass coverslips, paraffin-embedded tissue sections of eyes enucleated following failed retinal detachment surgery with PVR or sections of normal retina/RPE from eyes enucleated for choroidal melanoma, or surgically excised choroidal neovascular membranes were stained for uPAR using an avidin-biotinylated enzyme complex (ABC) technique. RPE cell preparations on coverslips were gently fixed for 5 minutes in 4% paraformaldehyde. Tissue sections were deparaffinized by immersing the sections sequentially in xylene, followed by graded alcohols. Endogenous peroxidase was blocked by preincubating the fixed RPE cell preparations or tissue sections in 0.3% H_2O_2 for 20 minutes. Nonspecific antibody binding sites were blocked using diluted normal blocking serum (Vectastain Universal Elite ABC kit, Vector Laboratories, Burlingame, California) for 20 minutes. Monoclonal antibody to uPAR (CD87; 1:25; American Diagnostica, Inc, Greenwich, Connecticut) was used as primary antibody. Platelet endothelial cell adhesion molecule-1 (PECAM-1; CD31), an antibody of similar isotype to uPAR, was used

as control primary antibody. Following a 30-minute incubation in primary antibody, sequential incubations of diluted biotinylated secondary antibody and Vectastain ABC reagent for 30 minutes each were performed (Vectastain Universal Elite ABC kit, Vector Laboratories, Burlingame, California). Reaction product was visualized by development in buffer containing 3-amino-9-ethylcarbazole (5 mg/mL) and 0.01% hydrogen peroxide to yield a red-brown, reaction product. Cell preparations were counterstained with hematoxylin and mounted in GelMount (Biomeda, Foster City, California).

NYLON-GEL MEMBRANE PREPARATION

Nylon mesh (Nytex-3-120/52, mesh opening 120 µm, Tetko Inc, Briarcliff Manor, New York) used for light microscopy and immunohistochemical studies was cut into 18-mm squares and rinsed in 75% ethanol for 5 minutes. Following drying under ultraviolet light for 30 minutes, the nylon mesh was placed in a 35-mm sterile Petri dish. A 4% gelatin solution was prepared by boiling gelatin in Hank's balanced salt solution (HBSS) and returning the gelatin solution to 37°C. Four drops (approximately 100 µL each) were placed on the nylon mesh and allowed to dry on a slide warmer at 42°C until tacky. One drop of 0.5% glutaraldehyde was then placed to the gelatin-nylon matrix and allowed to dry for 15 minutes on a slide warmer. Remaining glutaraldehyde was aspirated and the cross-linked gelatin-nylon mesh matrix removed with sterile forceps and rinsed three times in HBSS, each time for 10 minutes. To obtain more substantial gelatin-nylon mesh cell culture supports, the cross-linked gelatin was laminated by repeating the process of gelatin coating with the 4% gelatin solution and cross-linking with glutaraldehyde. Following final rinsing in HBSS, the gelatin-nylon mesh supports were placed in media in an incubator overnight to leach out any remaining glutaraldehyde. They were then rinsed and placed in 35-mm Petri dishes, and 25 µL of 10 mg/mL fibronectin solution was placed on their surfaces. The transportable, sterile cross-linked gelatin-nylon mesh matrices were allowed to dry for 20 minutes, following which RPE cells were seeded onto their surfaces in a dome-shaped drop that covered the nylon mesh. The RPE cells were allowed to attach to the mesh surfaces for 30 minutes at 37°C, following which the culture well was filled with the usual volume of regular media.

For cell migration and proteolysis studies, nylon mesh was cut into 12-mm squares and rinsed in 75% ethanol for 5 minutes. A 6% to 10% gelatin solution was prepared by boiling gelatin in HBSS containing either Bodipy-BSA (4,4-difluoro-5,7-dimethyl-4-bora-3a,4a-diaza-5-indacene-3-propionic acid-conjugated bovine serum albumin; Molecular Probes) or DQ collagen (type IV from human placenta, fluorescein conjugate; Molecular Probes Cat No. D-12052). Bodipy-BSA and DQ collagen were used to visualize proteolytic activity in the gel-mesh matrix. Bodipy-BSA and DQ collagen become fluorescent upon exposure to uPA protease activity and to collagenase activity, respectively.

To avoid denaturation of the Bodipy-BSA or DQ collagen added to the gelatin, the solution was allowed to cool to ~42°C before the addition of this compound. Ten microliters of cell attachment factor (Cell Systems Corporation, Kirkland, Washington) was placed on a coverslip for 15 minutes at 42°C in an incubator. After drying, a sterile nylon mesh was placed on the coverslip. Fifty microliters of 6% to 10% gelatin solution containing 10% fetal bovine serum (FBS) and Bodipy-BSA or DQ collagen (final concentration 1 mg/mL) was placed on the nylon mesh and allowed to harden in a refrigerator at 4°C for 10 minutes. The gelatin-nylon mesh matrix on the coverslip was then placed at room temperature.

HISTOCHEMICAL/IMMUNOHISTOCHEMICAL ANALYSIS OF NYLON MESH RPE CULTURES

RPE cultures grown on gelatin-nylon matrix were allowed to reach confluent monolayers. The cultures were monitored for confluence by observing them with phase contrast microscopy. Some cultures were then fixed with buffered 1% formaldehyde/0.5% glutaraldehyde and processed for light microscopy. For this, the cultures were sectioned with a razor blade, and portions were submitted for sequential dehydration through alcohols and embedding in plastic resin. Two-micrometer sections were then cut with a glass knife, stained with toluidine blue, and mounted on glass slides for light microscopic observation.

To detect RPE Na^+-K^+ ATPase membrane protein, immunoperoxidase staining was performed on 4-µm-section soft paraffin-embedded gelatin-nylon mesh RPE cultures.[109] Briefly, RPE sections were deparaffinized, rehydrated, and preincubated with blocking serum (10% goat serum) to avoid nonspecific binding. The sections were then incubated with primary rabbit-antibovine Na^+-K^+ATPase antibody (1:250 dilution, kind gift from Dr Steve Ernst, University of Michigan, Department of Anatomy and Cell Biology) for 1 hour. The sections were overlaid with 3% H_2O_2 for 5 minutes to block endogenous peroxidase activity and incubated sequentially with secondary biotinylated goat anti-rabbit antibody and streptavidin conjugated to horseradish peroxidase complexes (Dakopatts Immunoenzymatic Staining kit, DAKO Corp, Carpinteria, California). Tissue-bound antibody complexes were then visualized by development in a substrate solution containing 3-amino-9-ethyl carbazole (0.5 mg/mL; Sigma Chemical Co, St Louis, Missouri) and

0.01% H_2O_2 in 0.1 M acetate buffer, pH 5.2, to yield a granular, red-brown reaction product. The culture-preparation sections were fixed in 4% buffered formaldehyde and mounted in Gel/Mount (Biomedia Corp, Foster City, California). Negative controls included the use of normal rabbit serum (1:500) and preimmune rabbit immunoglobulin G (IgG) (1:250) in place of primary antibody.

FLUORESCENT STUDIES DEMONSTRATIN ASSOCIATION OF CD11B AND UPAR ON HUMAN RPE CELLS

Materials

Fluorescein isothiocyanate (FITC) and 7-amino-4-methyl-coumarin-3 acetic acid (AMCA) were obtained from Molecular Probes (Eugene, Oregon). Ethyl diaminotetra-acetic acid (EDTA) was obtained from Fisher Scientific Co (Fair Lawn, New Jersey). Fluorescein-conjugated uPA was obtained from American Diagnostica Inc (Greenwich, Connecticut).

Monoclonal Antibodies

Mouse monoclonal antibodies (mAbs) to CD11b (CR3), uPAR (clone 3B10), and their fragments were prepared as previously described.[111-117] Idiotypic antibodies for uPAR and CD11b were used as controls.

Preparation of FITC- and AMCA-conjugated Abs

The AMCA- and FITC-conjugated Abs were prepared as previously described.[118,119] The fluorescent conjugates were separated from unreacted fluorochromes by Sephadex G-25 (Sigma Chemical Co) column chromatography. Purified conjugates were dialyzed against PBS at pH 7.4 overnight at 4°C.

Fluorescence Labeling

RPE cells were detached from culture flasks by treatment with trypsin-EDTA. After detachment, the RPE cells were resuspended in culture medium supplemented with 10% FBS for 10 minutes at room temperature to inactivate any remaining trypsin activity. RPE in suspension was labeled with nonsaturating amounts of fluorochrome-conjugated $F(ab')_2$ fragments of anti-CD11b mAb for 20 minutes at 4°C. For capping experiments, the cells were washed twice with HBSS, then labeled with second-step goat anti-mouse IgG. Cells were incubated for 30 minutes at 37°C to allow cap formation. Cells were then labeled with $F(ab')_2$ fragments of anti-uPAR mAb for 20 minutes at 4°C followed by washing with cold buffer. After staining, the cells were washed with cold HBSS by centrifugation. Samples were then transferred to a microscope stage held at 37°C. These experimental manipulations had no apparent effect on cell activation for shape change as assessed by right-angle light scatter performed as described.[120]

Conventional Microscopy

An axiovert 135 inverted fluorescence microscope (Carl Zeiss Inc, New York, New York) with mercury illumination interfaced to a Perceptics Biovision workstation (Knoxville, Tennessee) was employed for cell examination. The fluorescence images were collected by an intensified charge-coupled device camera, model XC-77 (Hamamatsu, Japan) and image processor. Narrow bandpass discriminating filter sets were used for FITC (excitation at 485/22 nm and emission at 530/30 nm) and AMCA (excitation of 380/15 nm and emission at 450/30 nm)(Omega Optical, Brattleborrow, Vermont). Long-pass dichroic mirrors of 430 nm and 510 nm were used for AMCA and FITC, respectively. Digital images were collected using Zeiss polarizers and a charge-coupled device camera (model WV-BL200; Panasonic). The background-subtracted digitized images were averaged and then electronically stored. Fluorescence micrographs were prepared using the MultiProbe software package (Perceptics Inc, Knoxville, Tennessee) to pseudocolor and then overlay separate images of the same cell collected using different filter sets. Images were photographed using a freeze-frame video recorder (Polaroid, Boston, Massachusetts).

Resonance Energy Transfer (RET) Imaging

For RET microscopy,[121] the 485/22-nm narrow bandpass discriminating filter was used for excitation and the 590/30-nm filter was used for emission. The 510-nm long-pass dichroic mirror was used for RET.[117,121,122] Optical imaging was conducted as described in the preceding paragraph.

STUDIES OF RPE CELL MIGRATION

Human RPE Cell Preparation for Transmigration Studies

Human RPE (HPRE) cells were detached from culture flasks by treatment with trypsin-EDTA. After detachment, the RPE cells were resuspended in HBSS supplemented with 10% FBS for 10 minutes at room temperature to inactivate any remaining trypsin activity. After centrifugation at 1,000 rpm for 5 minutes, RPE cells were resuspended in HBSS at a concentration of 5×105 cells/mL. HRPE cells were stained by incubating with DiI (1,1'-dioctadecyl-3,3,3',3'-tetramethylindocarbocyanine; final concentration 20 µg/L) for 1 hour at 37°C with gentle agitation at 15-minute intervals. After labeling, the cells were washed twice by centrifugation and were seeded onto the surfaces of the gelatin-nylon mesh matrices in 50 µL of 6% gelatin solution containing 10% FBS. To visualize proteolytic activity, Bodipy-BSA (4,4-difluoro-5,7-dimethyl-4-bora-3a,4a-diaza-5-indacene-3-propionic acid-conjugated BSA; Molecular Probes) and DQ collagen (type IV from human placenta, fluorescein conjugate;

Molecular Probes Cat No. D-12052) were used. Bodipy-BSA becomes fluorescent on exposure to several proteases, especially uPA.[124] DQ collagen becomes fluorescent on exposure to collagenase activity. Bodipy-BSA or DQ collagen was incorporated into the gelatin-nylon mesh matrix layers at a concentration of 1 mg/mL. HRPE cells on the gelatin-nylon mesh matrices were incubated for 2 hours at 37°C in a 5% CO_2 incubator. The gelatin-nylon mesh matrices and coverslips were then mounted on glass slides for microscopic observation. The number of HRPE cells reaching the bottom surface of the matrix was divided by the number of cells added to the top layer to determine the fraction of cells that migrated across the matrix.

Inhibition of the Collagenase Activity

To inhibit metalloproteinase activity, 1,10-phenanthroline (Eluka Chemical Corp, Ronkonkoma, New York) was used.[125] During some of the preparation of the gel-nylon mesh matrices, 1,10-phenanthroline was incorporated into the matrix at a final concentration of 10 mM. Control gels contained only ethanol, the solvent used for 1,10-phenanthroline.

Inhibition of Urokinase-type Plasminogen Activator

To inhibit urokinase-type plasminogen activator, PAI-1 (American Diagnostica Corporation, Joplin, Missouri) was used. During preparation of some of the gel-nylon mesh matrices, PAI-1 was incorporated into the matrix at a final concentration of 0.05 mg/mL. Control gels contained only HBSS, the solvent used for PAI-1.

Fluorescence Microscopy and Image Reconstruction

An axiovert inverted fluorescence microscope (IM-135) with HBO-100 mercury illumination (Carl Zeiss Inc, New York, New York) interfaced to a Dell 410 workstation (Round Rock, Texas) via a Scion SG-7 video card (Vay-Tek, Fairfield, Iowa) was used. The fluorescence images were collected by an intensified, cooled charged-coupled device camera (model XC-77; Hamamatsu Photonics, Bridgewater, New Jersey). Images were processed with ScionImage software and stored as TIFF files. The fluorescence of Bodipy-BSA and DQ collagen fluorescence was detected using a 485DF22-nm and 530DF30-nm filter combination and a 510 long-pass dichroic mirror (Omega Optical, Brattleboro, Vermont).

For image reconstruction, images from 50 to 70 optical sections were taken from a sample. To remove out-of-focus fluorescence, each image was deconvoluted using MicroTome software (Vay-Tek). The three-dimensional rendering was performed with VoxBlast software (Vay-Tek). Computations were performed on a Dell Precision Workstation. Images were printed using an Epson Stylus-Pro printer.

Imaging Spectrophotometry

Fluorescence emission properties of the matrices were studied using imaging spectrophotometry. Experiments were performed as described previously.[126] Briefly, a Zeiss IM-135 axiovert microscope was fiber-optically coupled to the input side of an Acton-150 (Acton, Massachusetts) imaging spectrophotometer. The exit side was connected to an intensifier, which was in turn attached to a Peltier-cooled I-MAX-512 camera (Princeton Instruments, Inc, Trenton, New Jersey). The collection of spectra or images was controlled by a high-speed Princeton ST-133 interface and a DG-535 delay gate generator (Stanford Research Systems, Sunnyvale, California). This equipment was interfaced to a Dell 410 workstation running Winspec/32 version 2.3.2.5 software (Princeton Instruments, Inc) to manage image acquisition, quantitate fluorescence levels, and analyze data. Cells were illuminated using an optical filter at 485DF22 nm and a 5101p dichroic mirror.

PROCEDURES FOR ENZYMATIC FLUORESCENCE MICROSCOPY

Bodipy FL-BSA and DQ FL-Collagen IV Overnight Incubation Protocol

Slides were prepared by dissolving Bodipy-BSA FL conjugate (6%, Molecular Probes, Eugene, Oregon), bovine serum albumin (10%, Sigma, St Louis, Missouri), and D-collagen FL conjugate (12% 90, type IV from human placenta, fluorescein conjugate; Molecular Probes) in water. In some experiments human PAI-1 (5 ng/mL) (American Diagnostica, Greenwich, Connecticut) or 1,10-phenanthroline (10 mM) was added. This solution was evenly coated onto glass slides using a glass rod. The coated slides were incubated for 2 hours at 37°C in a humidified chamber. Following incubation, the slides were dipped in HBSS. The cell suspensions were then layered on top of the coated slides and allowed to adhere for 30 minutes at 37°C in a humidified box. The slides were dipped in HBSS to remove nonadherent cells, coverslips were added, and then samples were returned to the humidified box and incubated for 37°C for 8 to 16 hours. Where indicated, PAI-1 (5 ng/mL) or 1,10-phenanthroline (10 mM) was added to the cell suspension mixture immediately prior to layering the cells onto the coated slides.

Bodipy FL-BSA Procedures for Intensified Microscopy

BSA (50 µg) and Bodipy FL-BSA (30 µg) DQ-collagen (60 µg) were dissolved in 20 µL of dimethyl sulfoxide (DMSO). After suspension in solvent, the entire solution volume was diluted to 0.5 mL. This stock solution could be stored for up to 1 week at 4°C. One hundred microliters of the stock solution was evenly coated onto acetone-cleaned glass coverslips and incubated for 2 hours at 37°C in a humid air atmosphere under a Petri dish (but not

allowed to dry). The coverslip was gently washed with HBSS.

Intensified Microscopy

Cells were observed using an axiovert inverted fluorescence microscope (Carl Zeiss, Inc, New York, New York) with mercury illumination interfaced to a Perceptic (Knoxville, Tennessee) Biovision image processing system. A long-pass dichroic mirror of 510 nm and a narrow bandpass discriminating filter (DF) set (Omega Optical, Brattleboro, Vermont) was used (excitation at 485 nm with a 22-nm bandpass and emission at 530 nm with a 30-nm bandpass) for FITC and Bodipy FL. The fluorescence images were collected with an intensified charge-coupled device camera (Genisys; Dage-MTI, Michigan City, Indiana). Digital photomicrographs were taken using Zeiss polarizers and a charge-coupled device camera (model 72, Dage-MTI). To distinguish extracellular from intracellular fluorescence, samples were stained with 0.5 mg/mL crystal violet as previously described.[127,128]

Single Cell Excitation Microspectrophotometry

Cell fluorescence was quantitated using an emission microspectrophotometer system. To minimize light losses, a Zeiss IM-135 axiovert microscope with a bottom port was employed. The bottom port was fiber-optically coupled with an efficiency near 1.0 to the input side of an Acton-150 (Acton, Massachusetts) imaging spectrophotometer. The exit side was connected to an intensifier that was attached to a Peltier-cooled I-MAX-512 camera (Princeton Instruments Inc, Trenton, New Jersey). The collection of spectra was controlled by a high-speed Princeton ST-133 interface and a Stanford Res System (Sunnyvale, California) DG-535 delay gate generator. This high-efficiency, high-sensitivity system allowed medium resolution emission spectra to be collected from individual cells in 1 second. These systems were interfaced to a Dell 410 workstation running Winspec software to manage and analyze data. Cells were illuminated using an optical filter at 485DF22 nm and a 5101p dichroic mirror.

STUDIES ON THE SECRETION OF NONLYSOSOMAL HYDROLASES BY RETINAL PIGMENT EPITHELIAL CELLS

Tissue Culture and Stimulation of Monkey RPE Cells

Monkey RPE cells were isolated and cultured by the same methods described above for human RPE cells. Cultured cells were either left unstimulated or stimulated with IL1-ß (0.02 ng/mL or 0.2 ng/mL) for 24 hours prior to collagenase and elastase studies. Monkey RPE cell cultures were preincubated with 1,10-phenanthroline (10 mM) to inhibit collagenase and elastase activity.

DNA Quantitation of RPE Cell Cultures

The DNA contents of the cultured cell monolayers scraped from each tissue culture flask were determined according to the method of LaBarca and Paigen.[129] Briefly, the cells grown in tissue culture flasks were scraped into distilled water in the cold, briefly sonicated, and maintained on ice until DNA assays were performed. Twenty-five to 100-µL aliquots of the cell lysates, raised when necessary to a total of 100 µL by adding distilled water, were then added to 4.7 mL of a phosphate-saline buffer solution (0.05 M Na_3PO_4, 2.0 M NaCl) followed by addition of 0.5 µg of Hoechst 33258, a fluorescent dye which quantitatively binds to double-stranded DNA, in 200 µL of distilled water. The samples were then mixed vigorously and kept in the dark until fluorescence was measured using a Beckman Fluorocolorimeter with a 370-nm narrow-band interference filter for the excitation light and a Kodak 2A cutoff filter for light emission. Calf thymus DNA standards were used in each assay.

Determination of Collagenase Activity in RPE-Conditioned Media and Cell Layers

The collagenolytic activities of aliquots of RPE cell lysates were determined according to the method of Hu and associates[130] as modified by New England Nuclear for marketing as the "Collagenase Assay System [^{3}H]" (Cat No. NEK-016). Briefly, [^{3}H]-collagen fibrils were formed in chilled reaction tubes in 2.0 mM Tris HCl buffer, pH 7.6, containing 5.0 mM $CaCl_2$ for 2 hours before cell lysates were added. Forty microliters of cell lysate in distilled water was then added to the reaction tubes and incubated in the presence of 0.5 mM 4-aminophenylmercuric acetate for 24 hours at 25°C under gentle agitation to assay for both active and latent collagenase activity. Following incubation, the reaction tubes were centrifuged at 15,000*g* for 7 minutes at 25°C to separate the uncleaved collagen fibrils from the cleaved fragments in the supernatants. Twenty-microliter aliquots of the supernatants were removed and counted in aqueous counting solution (Awasol, New England Nuclear, Boston, Massachusetts). Samples from each culture flask were assayed in duplicate. Tissue culture flasks were run in triplicate for each culture condition. Control samples of nonconditioned media, media containing 0.5% trypsin and buffer, and media incubated with 1,10-phenanthroline (10 mM) for 30 minutes at 20°C were also assayed. The results are recorded as counts per minute/µg DNA.

Determination of Elastase Activity in RPE-Conditioned Media and Cell Layers

Radioactive [^{3}H]-elastin prepared according to Banda and Werb[131] was supplied by Dr Harry Davis. The elastase activity was measured by determining the amount of radioactivity released after incubation of 100 µL of each cell lysate at 37°C with 200 µg of [^{3}H]-elastin in 100 mM

Tris-HCl buffer, pH 7.8, containing 5 mM $CaCl_2$ and 0.2% $NaNO_3$. The lysates and [^{3}H]-elastin were allowed to incubate for 48 hours at 37°C. At the end of incubation, assay tubes were centrifuged for 3 minutes at 15,000*g* in a Beckman microfuge. The radioactivity in a 100-µL aliquot of the supernatant was measured by liquid scintillation spectrometry. Samples from each culture flask were assayed in duplicate. In separate assays, tissue culture flasks were run in triplicate for each culture condition. Control samples of nonconditioned media, media containing 0.5% trypsin buffer, and media incubated with a broad metalloproteinase inhibitor 1,10-phenanthroline (10mM) for 30 minutes at 20°C were also assayed. The results are recorded as counts per minute/µg DNA/hour.

STATISTICAL ANALYSIS

For comparisons, unpaired Student's *t* tests were performed. Data are expressed as mean ± standard error of the mean (SEM). Differences were considered significant at $P<.01$. All experiments were repeated on at least three independent occasions.

RESULTS

IMMUNOHISTOCHEMICAL STAINING OF HUMAN RPE CELLS IN VITRO AND IN SITU

Immunohistochemical staining of cultured human RPE cells demonstrated constitutive (Figure 1A) staining, which was completely blocked by preadsorption of antibody with purified uPAR (Figure 1B). Proinflammatory cytokines, IFN-γ (100U/mL; Figure 1C), and TNF-α (0.2 ng/mL)(not shown) enhanced immunoreactive uPAR expression on human RPE cells. Lipopolysacchride also induced substantial increased uPAR immunoreactivity (Figure 1D). The proinflammatory cytokine, IL-1ß, also induced dose-responsive increases in immunoreactive uPAR expression (Figure 2). In all cases, diffuse red-brown granular reaction product was present, with increased density of reaction product noted along cell membranes at high power (Figure 2D). Enhanced perinuclear staining was also evident in unstimulated as well as proinflammatory cytokine and LPS-stimulated cells. Human RPE cells stained with control antibody, PECAM-1, failed to show any immunoreactivity (Figure 2B).

In situ immunohistochemical staining for uPAR in formalin, paraffin-embedded sections of human eyes revealed immunoreactive uPAR to be distributed throughout the RPE cytoplasm with enhanced expression along RPE basolateral membranes (Figure 3A). Immunofluorescent staining of live, confluent cultures of human RPE cells (Figure 4A) demonstrated immunopositivity for CD11b/CD18 (Figure 4B), as previously described,[101,132] which was similar in distribution to that of uPAR (Figure 4C). Noteworthy was enhanced perinuclear immunofluorescence present around the nuclei for both receptors, mimicking the staining on the fixed cell cultures (Figures 1 and 2). Simultaneous immunofluorescent staining on human RPE for uPAR and CD11b/CD18 was viewed by high-speed photomicroscopy and confirmed the close association of these receptors, inferred from the similar patterns of immunoreactive staining observed in Figure 5. Using anti-uPAR and anti-CD11b monoclonal antibodies, each labeled with a separate fluorochrome, interspersed immunoreactivity for uPAR (yellow-green) with that of CD11b (blue) was readily observed in spherical (nonpolarized) RPE cells along the circumference of the cells (Figure 5A). Resonance energy transfer between the two fluorochromes (red) yielded photochemical confirmation of the proximity of the two receptors to within 8 nm of each other (Figure 5A) (Table II; $P<.01$). In contrast, elongated (polarized), motile-appearing RPE cells exhibited segregation of the receptors with uPAR migrating to the leading edge (lamellipodia) and CD11b to the trailing edge (uropodia) (Figure 5A). This resulted in concentration of all uPAR immunoreactivity at the leading poles of the polarized RPE cells (Figure 5A).

RPE HYDROLYSIS OF ALBUMIN, COLLAGEN IV, COLLAGEN III, AND ELASTIN

To demonstrate functional uPAR expression in RPE cells, the RPE cells were seeded onto slides coated with gelatin containing BSA labeled with a fluorochrome (Bodipy), which only exhibits fluorescence upon albumin lysis. RPE pericellular fluorescence was evident surrounding virtually all RPE cells and was significantly reduced ($P<.001$) by inclusion of PAI-1 in the assay (Figure 6). uPAR activity was significantly increased ($P<.001$) when RPE cells were exposed to IL-1ß (0.2 ng/mL) for 24 hours. PAI-1 significantly inhibited ($P<.001$) IL-1 ß–induced uPAR lysis of BSA (Figure 6).

To show the ability of RPE cells to cleave type IV collagen, known to be a component of Bruch's membrane, immediately underlying the RPE layer in vivo, RPE cells were seeded onto slides coated with gelatin containing collagen labeled with a fluorochrome (DQ), which only becomes fluorescent upon collagen lysis. As in the case of uPAR, pericellular proteolysis was seen around each RPE cell and was inhibited by the broad metalloproteinase inhibitor, 1,10-phenanthroline (10 mM) ($P<.001$). However, in contrast to uPAR, IL-1 ß (0.2 ng/mL) did not induce type IV collagenolysis by RPE cells over that observed surrounding unstimulated RPE cells (Figure 7). To demonstrate RPE hydrolytic activity for native interstitial collagen and elastin present within the inner lamellae of Bruch's membrane, assays employing radiolabeled

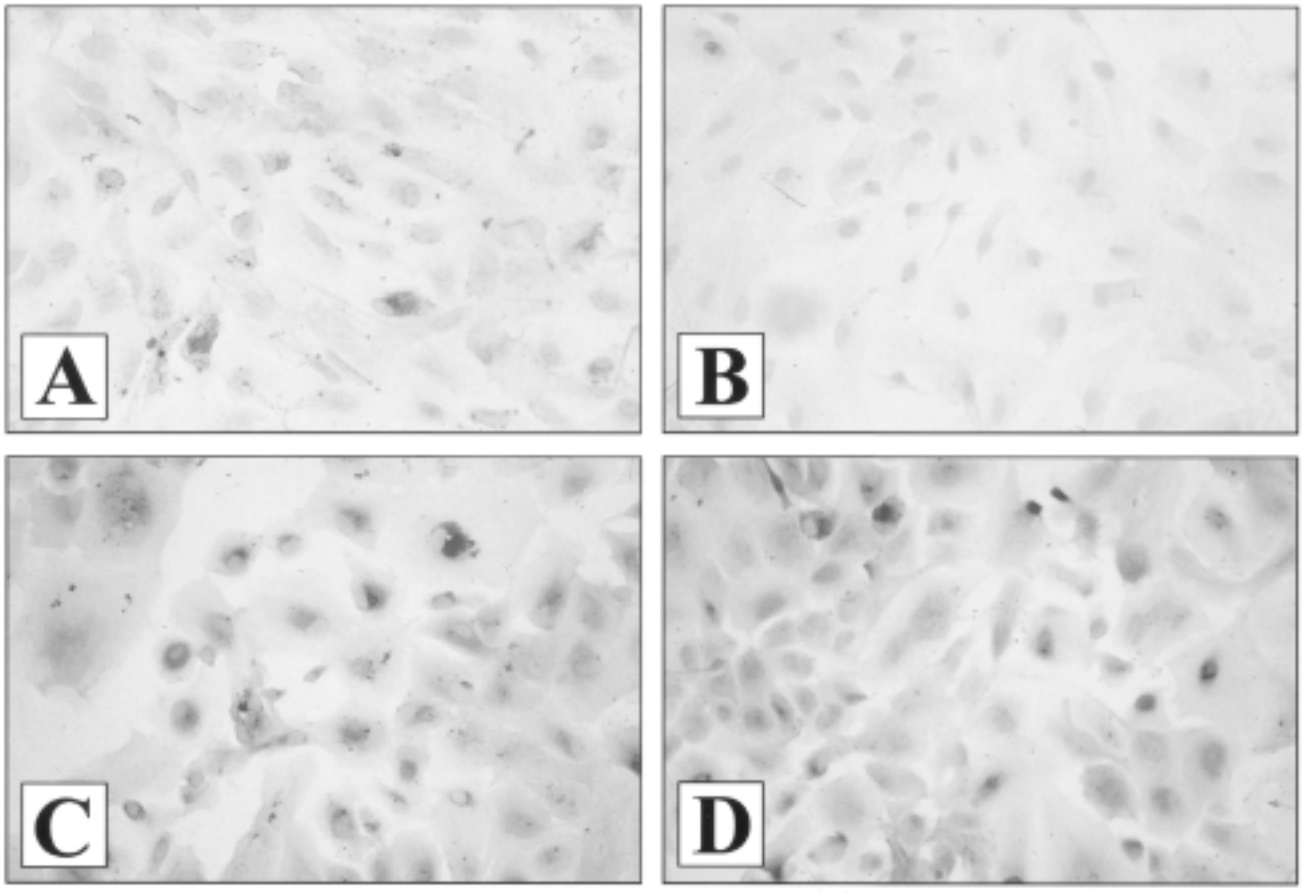

FIGURE 1
Immunohistochemical staining of nearly confluent, cultured human RPE cells for uPAR. A, Unstimulated RPE cells demonstrate predominantly perinuclear red-brown reaction product with other portions of cells lightly stained (hematoxylin counterstain, x200). B, Unstimulated RPE cells with anti-uPAR antibody preadsorbed with excess soluble uPAR show no detectable stain (hematoxylin counterstain, x200). C, RPE cells stimulated with interferon-gamma (100 U/mL) show heavy red-brown perinuclear stain as well as lighter diffuse stain (hematoxylin counterstain, x200). D, RPE cells stimulated with lipopolysaccharide (100 ng/mL) show marked increase in uPAR expression similar in distribution to that induced by interferon-gamma (hematoxylin counterstain, x200).

collagen III fibrils and radiolabeled native elastin were performed (Figures 8 and 9, respectively). Constitutive RPE hydrolysis of collagen III into classic 1/4 to 3/4 fragments was measured and significantly inhibited by 1,10-phenanthroline (Figure 8). Dose-dependent induction of collagenolytic activity resulted in significantly increased hydrolysis of collagen fibrils by RPE cells stimulated with IL-1ß (0.2 ng/mL)(P<.001). The proinflammatory cytokine-induced collagen III lysis was significantly inhibited by 1,10-phenanthroline (P<.001). Elastolytic activity secreted by RPE cells demonstrated similar constitutive and IL-ß-induced profiles (Figure 9). Baseline elastin hydrolysis was significantly inhibited by 1,10-phenanthroline (P<.001) and augmented by IL-1ß in a dose-dependent fashion with significantly increased secreted elastolytic activity induced by IL-1ß (0.2 ng/mL) (P<.001). As with the collagenolytic activity, 1,10-phenanthroline significantly inhibited the cytokine-induced activity (P<.001). Nonconditioned media and trypsin and buffer control samples degraded less than 5% of the collagen fibrils.

RELATIVE CONTRIBUTIONS OF RPE EXTRACELLULAR MATRIX PROTEOLYTIC ACTIVITY TO RPE MIGRATION

To demonstrate the relative contributions of RPE-associated collagen IV, collagen III, and elastin proteolysis and of RPE uPAR-mediated proteolysis to RPE migration through extracellular matrix, three-dimensional matrices were constructed as previously described.[133] RPE cells were seeded onto fibronectin-coated matrices composed of collagen gel enveloping sheets of 120-µm nylon mesh and grown to confluency (Figure 10). Confluent RPE cells on the matrices demonstrated typical polygonal arrays (Figures 10A and 10B), produced melanin (Figure 10C), and exhibited polarity with the formation of apical microvilli (Figure 10D). Immunohistochemistry for sodium-potassium-ATPase confirmed the RPE polarity by preferential immunopositivity at the cell apices (not shown).

RPE cells seeded onto Bodipy-BSA or DQ collagen-

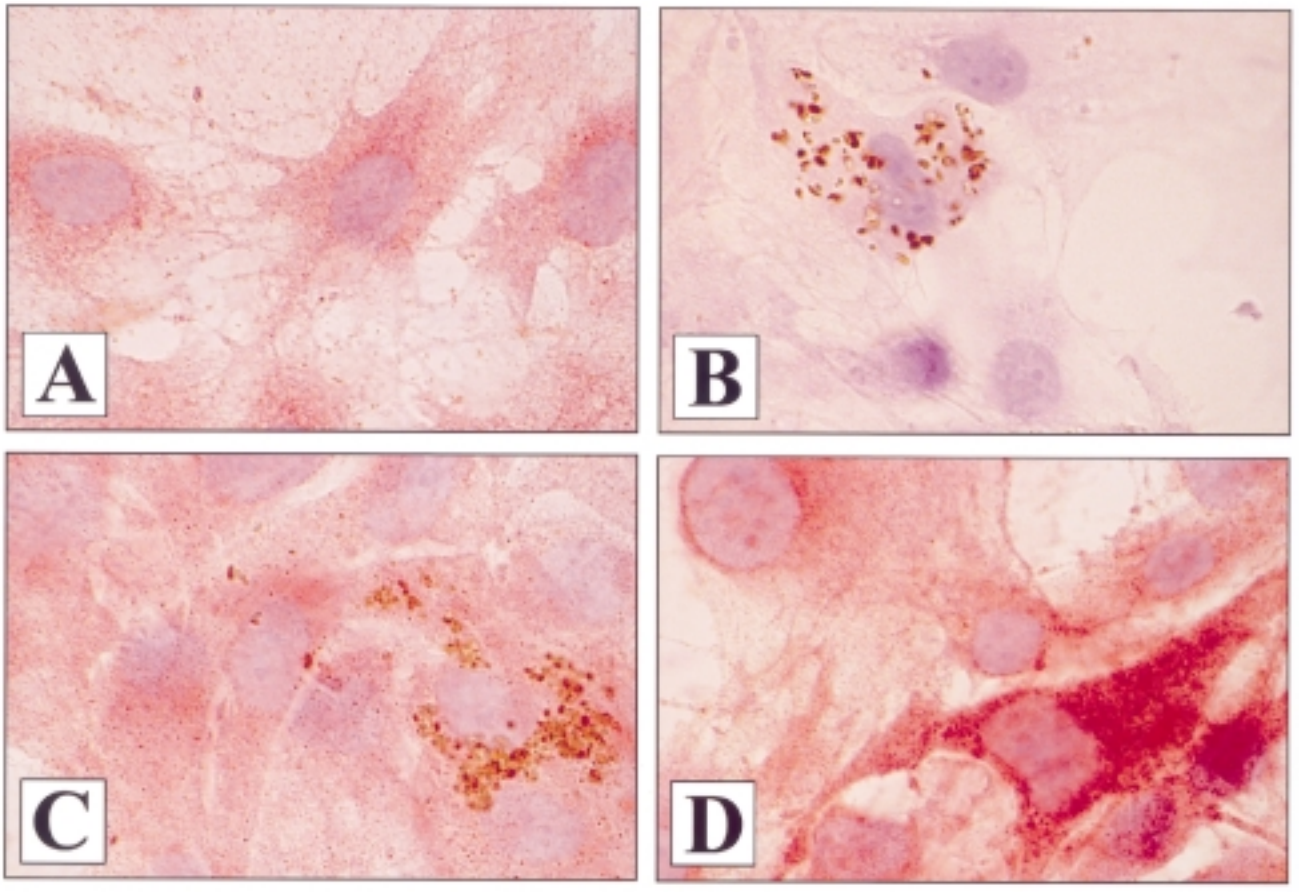

FIGURE 2

Immunohistochemical staining of nearly confluent, cultured human RPE cells for uPAR after exposure to interleukin-1ß. A, Unstimulated RPE cells stained for uPAR demonstrate diffuse mild staining with increased positivity in the perinuclear region (hematoxylin counterstain, x1,000). B, Unstimulated RPE cells show no stain using idiotypic control antibody. Prominent melanin granules are visible in an RPE cell (hematoxylin counterstain, x1,000). C, RPE stimulated with 0.02 ng/mLof interleukin-1ß exhibit more intense, diffuse deposition of red-brown reaction product when compared to unstimulated cells (hematoxylin counterstain, x1,000). D, RPE cells exposed to 0.2 ng/mL of interleukin-1ß are heavily stained with red-brown reaction product that is enhanced in the perinuclear regions (hematoxylin counterstain, x1,000).

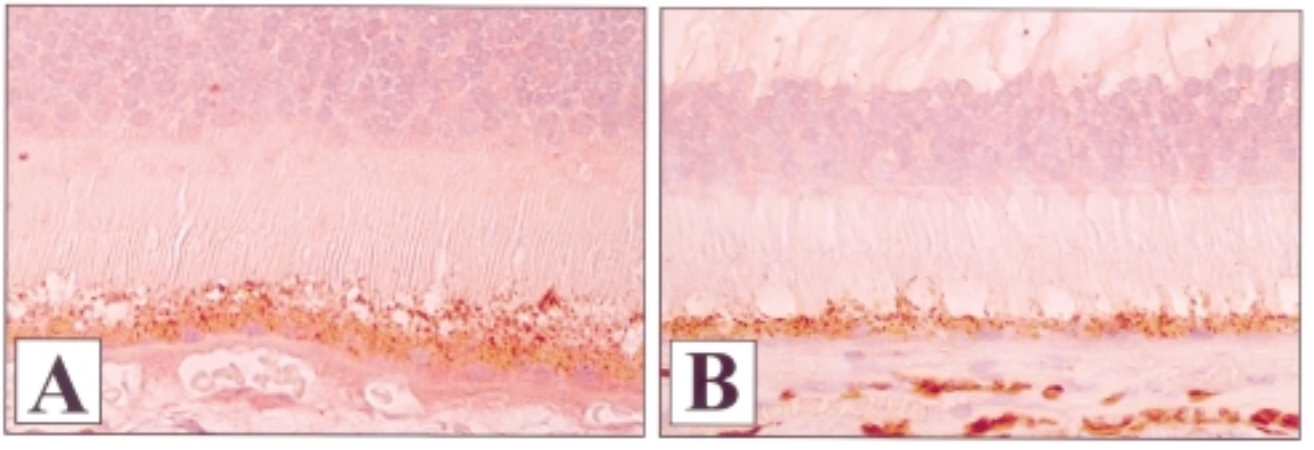

FIGURE 3

Immunohistochemical staining of normal human outer retina and choroid for uPAR. A, Red-brown immunohistochemical staining is present in RPE monolayer and demonstrates increased positivity along RPE basolateral membranes (hematoxylin counterstain, x1,000). B, Immunohistochemical staining performed using idiotypic control antibody fails to reveal any reaction product (hematoxylin counterstain, x1,000).

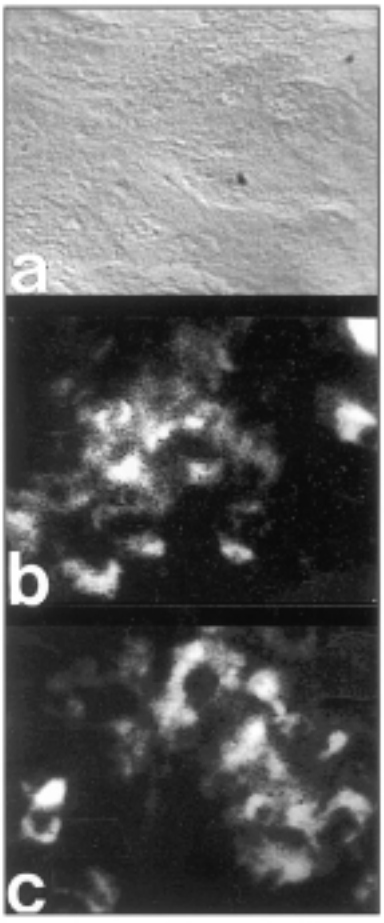

FIGURE 4

Immunofluorescent staining of live, confluent human RPE cultures for CD11b and uPAR. A, Phase contrast photomicrograph of confluent RPE cells (x400). B, Immunofluorescent staining for CD11b demonstrates diffuse membrane positivity with enhanced perinuclear immunufluorescence, mimicking results of fixed cell cultures stained for uPAR (x400). D, Immunofluorescent staining for uPAR demonstrates diffuse and enhanced pericellular distribution similar to that of CD11b (x400).

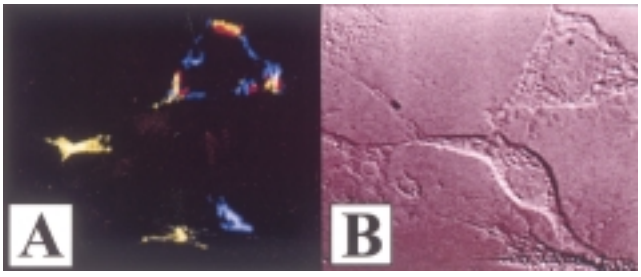

FIGURE 5

Live human RPE cells demonstrating CD11b (blue fluorescence) and uPAR (green fluorescence) due to binding of F(ab')2 fragments of specific anti-CD11b and anti-uPAR monoclonal antibodies. A, Polygonal RPE cell (upper right) demonstrates circumferential, interspersed CD11b and uPAR with red fluorescence indicating resonance energy transfer (RET) between blue and green fluorochromes due to close approximation of CD11b and uPAR. Elongated RPE cells (lower left) demonstrate segregation and concentration of uPAR at leading edge of cell with concentration of CD11b at trailing edge. No RET is present in the elongated cells (x1,000). B, Phase contrast photomicrograph of same microscopic field depicted in A (x1,000).

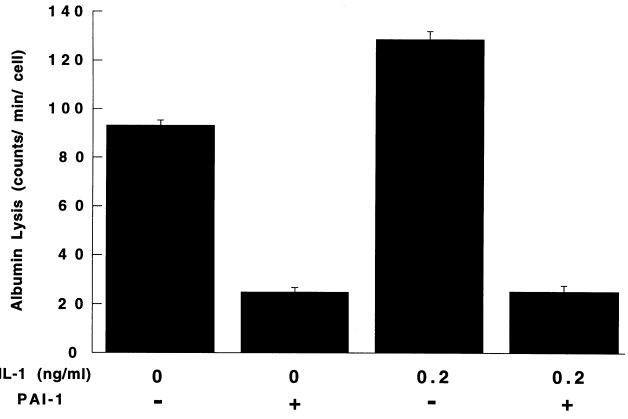

FIGURE 6

Human RPE lysis of albumin due to uPAR activity. Unstimulated and IL-1-stimulated RPE cells were assessed for pericellular proteolysis of albumin using Bodipy-BSA substrate. RPE cells exhibited constitutive activity, which was significantly enhanced by IL-1ß (0.2 ng/mL) (P<.001) and significantly inhibited by plasminogen activator inhibitor-1 (PAI-1) (P<.001).

TABLE II: ASSOCIATION OF RPE uPAR AND CR3

CELL CONDITION	NO. OF CELLS	INTENSITY OF RESONANCE ENERGY TRANSFER FLUORESCENCE (COUNTS/SEC)	*P*
CR3-to-uPAR RPE-spherical (not polarized)	35	326±36 x 10^3	<.01
CR3-to-uPAR RPE-elongated (polarized)	25	51±14 x 10^3	<.01

RPE, retinal pigment epithelium.

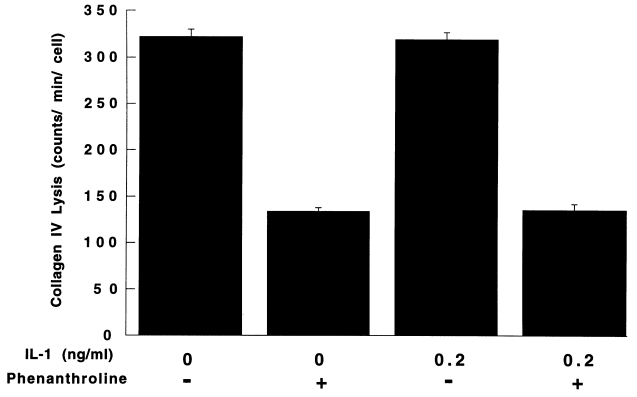

FIGURE 7

Human RPE lysis of collagen IV. Unstimulated and IL-1-stimulated RPE cells were assessed for pericellular proteolysis of collagen IV using DQ collagen substrate. RPE cells showed constitutive activity, which was significantly enhanced by IL-1ß (0.2 ng/mL) (P<.001) and significantly inhibited by 1,10-phenanthroline, a broad-spectrum metalloproteinase inhibitor (P<.001).

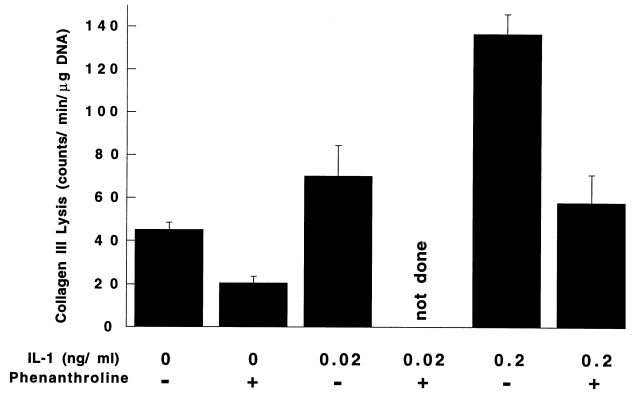

FIGURE 8

Human RPE lysis of collagen III. Supernatants from unstimulated and IL-1-stimulated RPE cells, activated with trypsin, were assessed their ability to cleave radioactively labeled collagen III fibrils. RPE cells showed constitutive activity which was significantly enhanced by IL-1ß (0.2 ng/mL) (P<.001) and significantly inhibited by 1,10-phenanthroline, a broad-spectrum metalloproteinase inhibitor (P<.001). IL-1ß at lower dose (0.02 ng/mL) demonstrated increases in hydrolytic activity that were not statistically significant.

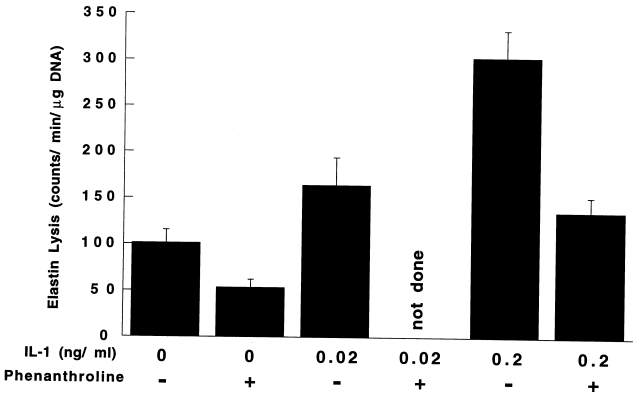

FIGURE 9

Human RPE lysis of elastin. Supernatants from unstimulated and IL-1–stimulated RPE cells, activated with trypsin, were assessed their ability to cleave radioactively-labeled native elastin. RPE cells showed constitutive activity which was significantly enhanced by IL-1ß (0.2 ng/mL) (P<.001) and significantly inhibited by 1,10-phenanthroline, a broad spectrum metalloproteinase inhibitor (P<.001). IL-1ß at lower dose (0.02 ng/mL) demonstrated increases in hydrolytic activity that were not statistically significant.

containing matrices readily migrated through the gels over 2 hours. Both fluorochromes were cleaved from the BSA or collagen as RPE migrated through the gels as depicted three-dimensionally (Figures 11A and 11B, respectively). Localized, intense RPE pericellular fluorescence was present at the site of active cleavage of the gels by the migrating RPE cells. Behind the migrated RPE cells, diffusing, cleaved fluorescent protein fragments diffused through the gels from the axes of RPE penetration, resulting in tails of weak fluorescence that expanded and dissipated with time (Figures 11A and 11B). Observations made during the RPE migration assays revealed that RPE cells on the gel surface adjacent to axes of penetration migrated to reach these axes in order to penetrate the gel rather than bore their own paths (data not shown).

To assess the role of RPE uPAR opposed to the secreted RPE collagenolytic and elastolytic that were measured in this study, RPE migration assays were performed in the presence and absence of PAI-1 and in the presence and absence of 1,10-phenanthroline. PAI-1 virtually abolished RPE cell migration through the collagen matrices (P<.001) (Figure 12A), while 1,10-phenanthroline, a known inhibitor of a wide spectrum of metalloproteinases and of the collagenases and elastases that were measured in this study, failed to demonstrate any inhibition of RPE cell migration (Figure 12B). These observations indicate a preeminent role of uPAR in RPE migration through extracellular matrix.

IMMUNOHISTOCHEMICAL DETECTION OF uPAR IN HUMAN RETINAL LESIONS

The presence of uPAR was confirmed in retinal lesions, characterized by disruptions in Bruch's membrane, RPE migration and proliferation, and inflammation. Examined were tissues or whole eyes with subretinal neovascular membranes (Figures 13 and 14), which emerge from the choroid through breaks in Bruch's membrane, proliferative vitreoretinopathy membranes containing migrated RPE cells (Figure 15), and eyes with end-stage uveitis (Figure 16). In whole eyes, subretinal neovascular membranes were frequently lined by RPE cells extending from Bruch's membrane over the vanguard. In surgically

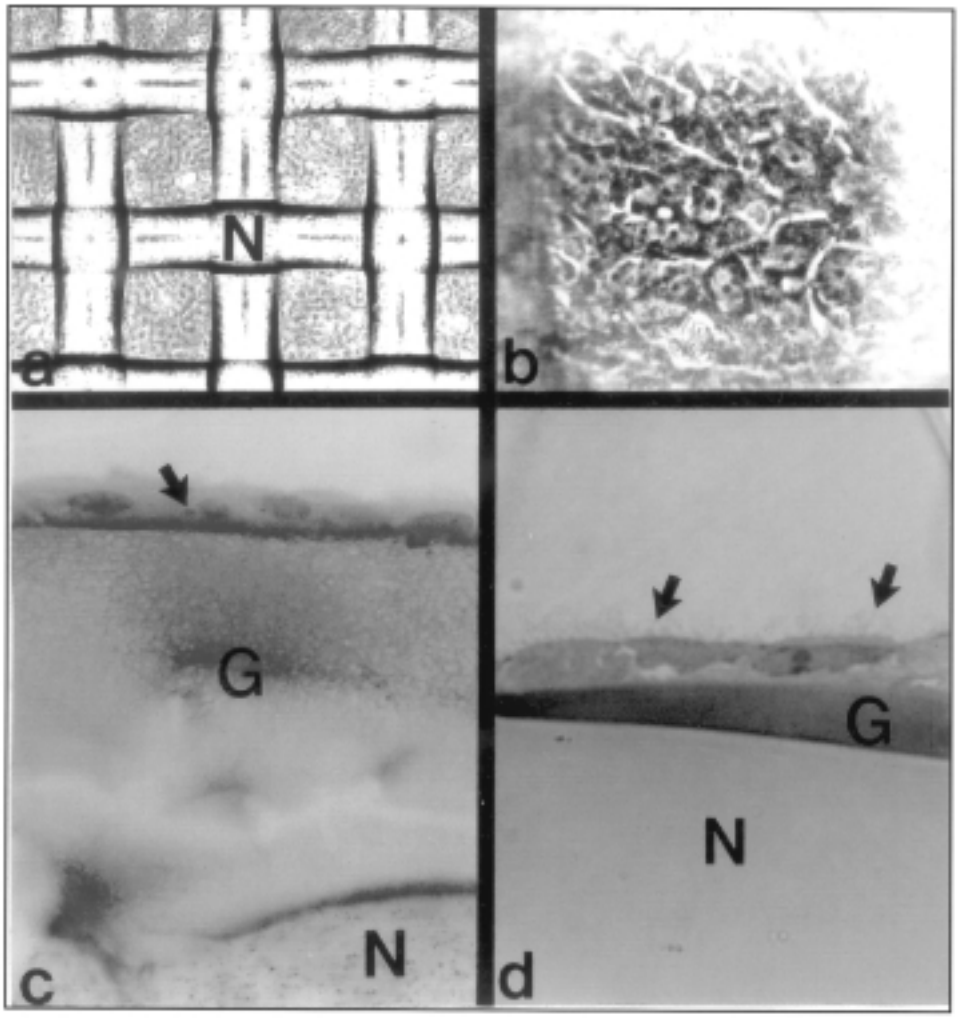

FIGURE 10

Human RPE cells cultured on novel, fibronectin-coated, gelatin/nylon (N) mesh. A, Inverted phase photomicrograph of RPE cells seen between strands of mesh exhibit typical polygonal arrays (x25). B, High-magnification photomicrograph demonstrating compact polygonal arrays of RPE cells (x200). C, Photomicrograph of formalin-fixed, paraffin-embedded section of gelatin (G)/nylon (N) mesh with confluent RPE monolayer demonstrates intracellular pigment granules (hematoxylin counterstain, x200). D, Formalin-fixed, plastic embedded gelatin(G)/nylon (N) mesh with RPE monolayer exhibiting polarization with formation of apical microvilli (arrows) (toludine blue, x400).

excised specimens, corresponding caps of readily identifiable RPE cells lined the surfaces of the fibrovascular membranes (Figures 13 and 14). These cells exhibited intense immunoreactivity for uPAR (Figures 13A and 14A). Some endothelial cells within the fibrovascular proliferations also stained positively, as did occasional mononuclear phagocytes. Serial sections stained with control antibody failed to show significant stain.

PVR membranes were characterized by RPE cells enmeshed in connective tissue of variable densities. RPE proliferations were frequently in cords, nests, or glandular configurations (Figure 15). Mild to moderate staining was seen multifocally in many of these proliferations, with immunoreactivity also present in the pericellular stroma (Figure 15).

Immunohistochemical staining of eyes with uveitis demonstrated immunoreactivity in the RPE monolayers and exudates overlying the choroidal inflammatory lesions. This polarized immunoreactivity was more intense than the degree observed to be constitutively present (Figure 3). Weaker but distinct immunoreactivity was exhibited by leukocytes within the choroidal lesions, as well as by some of the choroidal endothelium (Figure 16).

DISCUSSION

Mechanisms mediating RPE motility through the ECM in retinal lesions of ARMD, PVR, and uveitis remain largely unknown. Based on immunohistochemical, gene expression, and immunochemical observations, MMP and uPAR/uPA activity has been attributed to the

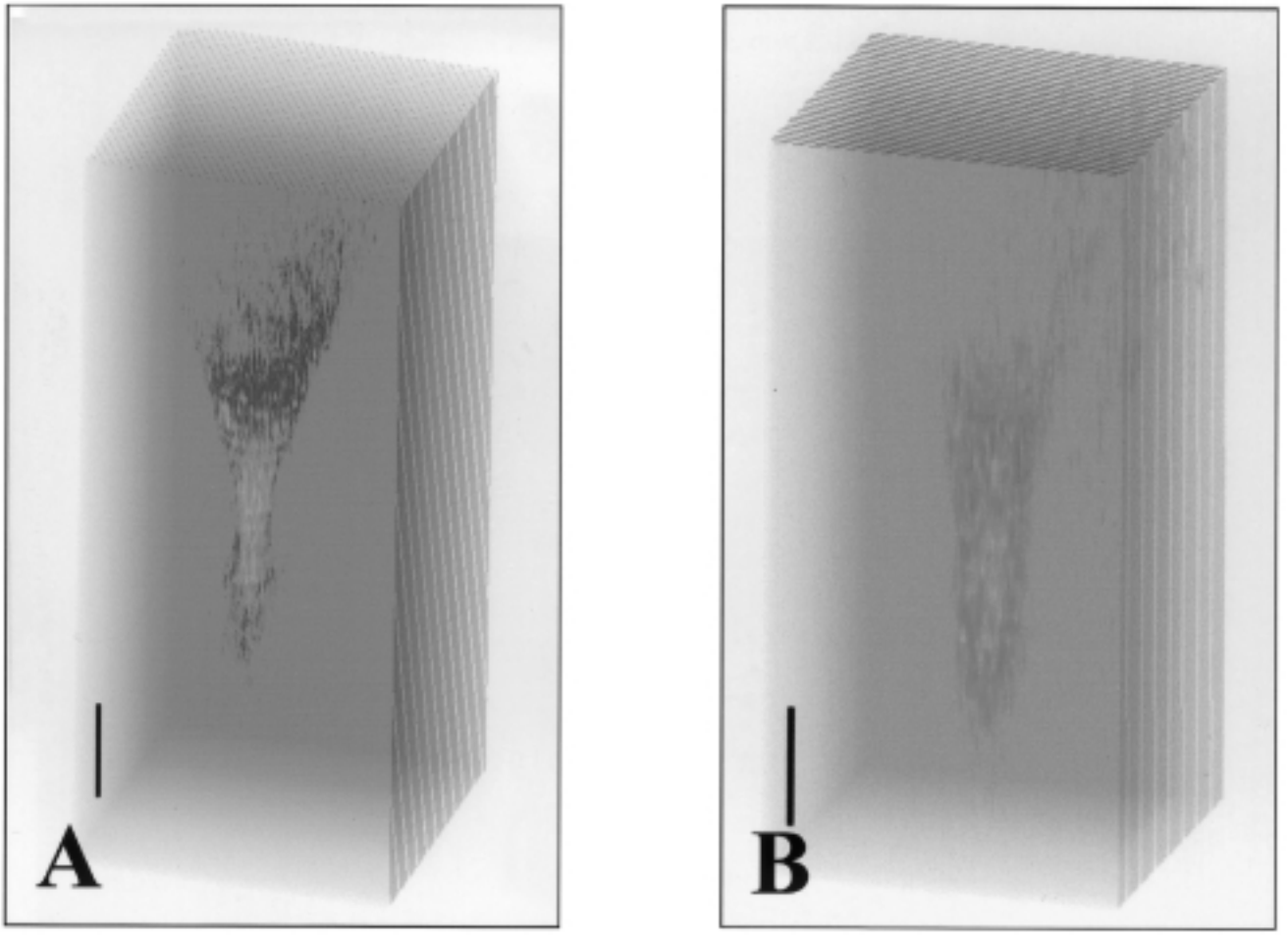

FIGURE 11

Three dimensional images showing RPE transmigration through gelatin/nylon mesh. A, Three-dimensional image reconstructed from multiple images acquired during migration of RPE cell through gelatin/mesh containing Bodipy BSA shows fluorescent fragments generated due to BSA cleavage by penetrating RPE cell. Concentration of fluorescence is seen where cell is cleaving albumin with a widening plume of fluorescence seen behind cell due diffusion of cleaved product from areas of prior cleavage (scale bar, 20 μm). B, Three-dimensional image of RPE transmigration using DQ collagen (collagen IV) substrate (scale bar, 20 μm).

RPE.[59,60,62,63,83,84,134,135] However, demonstration of uPAR immunoreactivity in RPE cells in vitro and in situ and the upregulation of RPE uPAR in response to proinflammatory cytokines that are known to be present in retinal lesions of ARMD, PVR, and uveitis have not been shown. Moreover, functional assays demonstrating actual uPAR-mediated proteolysis, its specific inhibition, its regulated expression on the RPE cell surface, and its role in RPE motility have not been investigated. With respect to MMP, this is the first study to show actual cleavage of native interstitial collagen, elastin, and collagen IV by RPE MMPs and their upregulation by a proinflammatory cytokine. Of particular interest is the demonstration of the relative contribution of uPAR/uPA and MMPs in RPE migration as assayed in a novel gelatin–nylon mesh medium using fluorescently labeled RPE cells.

RPE uPAR expression is present constitutively in vitro (Figures 1 and 2) and in situ where it is expressed preferentially along the RPE basolateral membrane (Figure 3). RPE uPAR expression under normal conditions is not surprising, since many receptors are normally expressed, even though their functional expression may be tightly controlled under physiologic conditions. For uPAR, such control is likely to be due to the presence of PAI-1, which has been shown to be secreted by numerous cells in the posterior segment of the eye, including the RPE.[84] Other possible mechanisms include the activity of MMPs that are normally produced to participate in the orderly turnover of ECM, including Bruch's membrane, and are themselves regulated by TIMPs.[135] One MMP, stromelysin, may be of particular interest with respect to its variable effects on uPAR activity. MMP-3 can downregulate uPA/uPAR activity, since it can (1) cleave the active portion of uPAR required for uPA activation[105] and

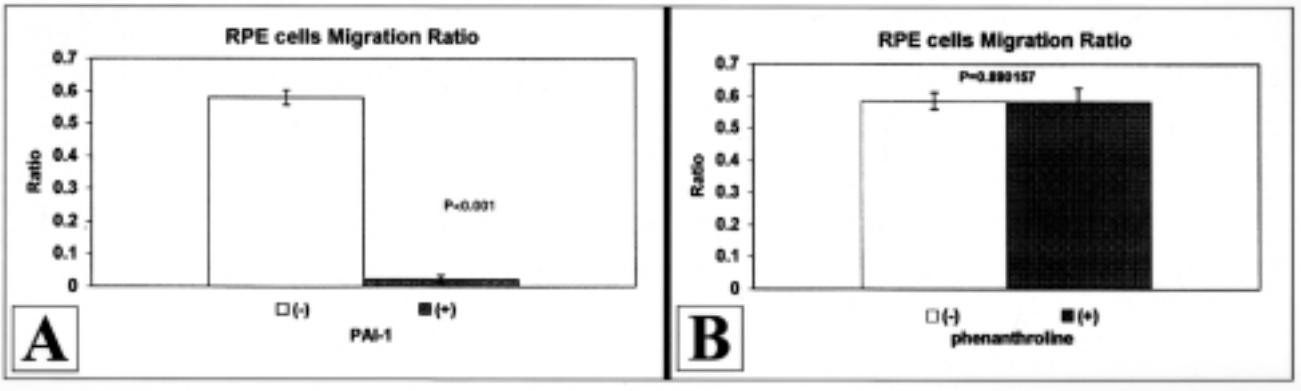

FIGURE 12

Effect of protease inhibitors on human RPE transmigration across the nylon-mesh gelatin matrices. The number of DiI, fluorescently labeled RPE cells reaching the bottom surface of the matrices after 4-hour incubations at 37°C was divided by the number of cells initially placed on top of the gelatin to determine the percentages of cells which migrated across the matrices. Experiments were performed in the presence (open bars) and absence (solid bars) of inhibitors. The uPAR/uPA inhibitor PAI-1 was found to profoundly inhibit cell migration (A), but the broad-spectrum metalloproteinase inhibitor, 1,10-phenanthroline, was found to have much less effect (B).

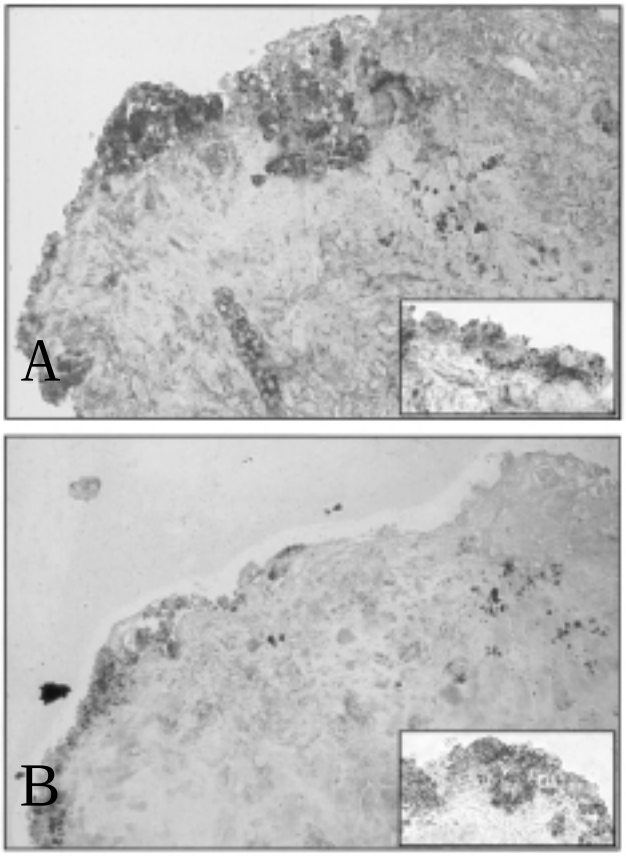

FIGURE 13

Immunohistochemical staining of surgically excised human subretinal neovascular membrane for uPAR. A, Readily identifiable RPE cells that line the surface of the membrane exhibit intense, red immunoreactivity. Some stromal cells, vascular endothelial cells, and leukocytes also show positivity. Inset shows readily visible red reaction product for uPAR (hematoxylin counterstain, x200; inset, x1,000). B, Adjacent tissue section stained using idiotypic control antibody lacks any immunoreaction (hematoxylin counterstain, x200).

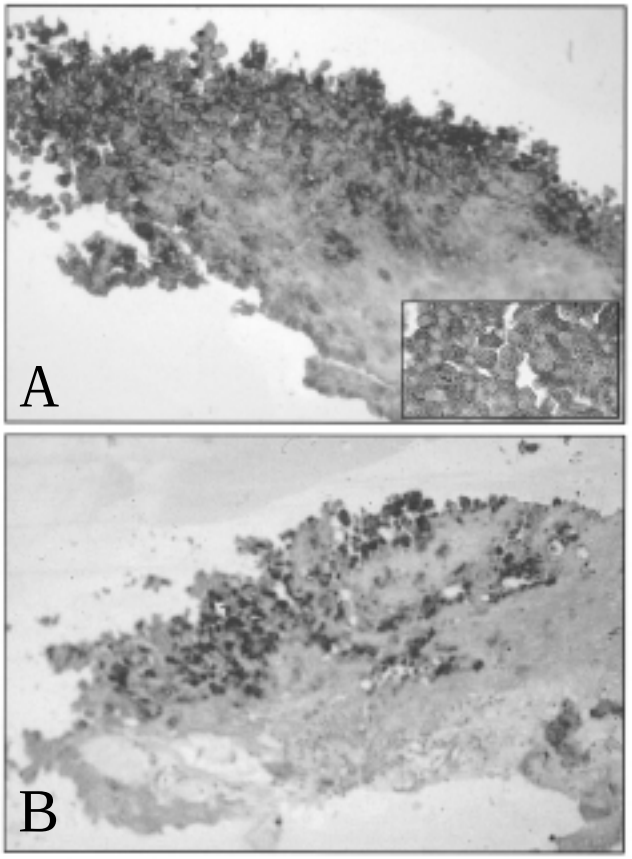

FIGURE 14

Immunodetection of uPAR in surgically excised human subretinal neovascular membrane. A, Numerous variably heavily pigmented polygonal RPE cells that occupy and line the surface of the membrane are intensely red due to uPAR immunoreactivity. Occasional stromal cells, endothelial cells, and leukocytes in the membrane also positively stained. Inset shows polygonal RPE cells decorated with deep red uPAR immunoreaction product (hematoxylin counterstain, x200; inset, x1,000). B, Adjacent tissue section stained using idiotypic control antibody is negative (hematoxylin counterstain, x200).

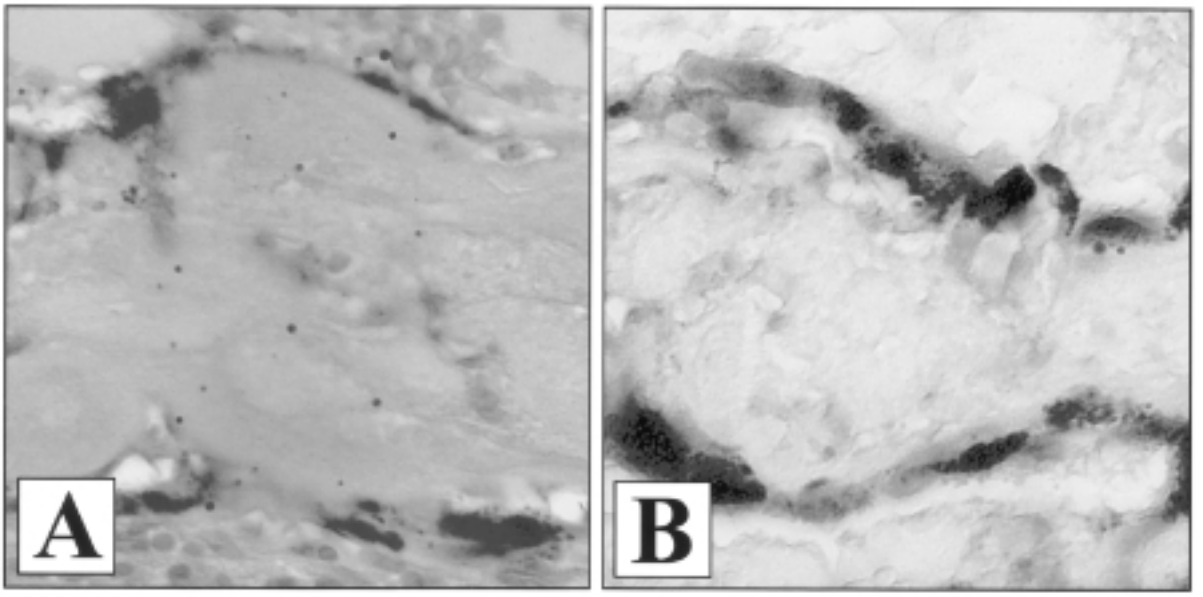

FIGURE 15

uPAR immunostaining in surgically excised human proliferative vitreoretinopathy membrane. A, Strands of infiltrating RPE cells present in moderately dense extracellular matrix of the membrane show immunoreactivity for uPAR. The stroma shows weak positivity, perhaps due to soluble uPAR in the lesion (hematoxylin counterstain, x400). B, Adjacent tissue section stained with control monoclonal antibody lacks any immunohistochemical positivity (hematoxylin counterstain, x400).

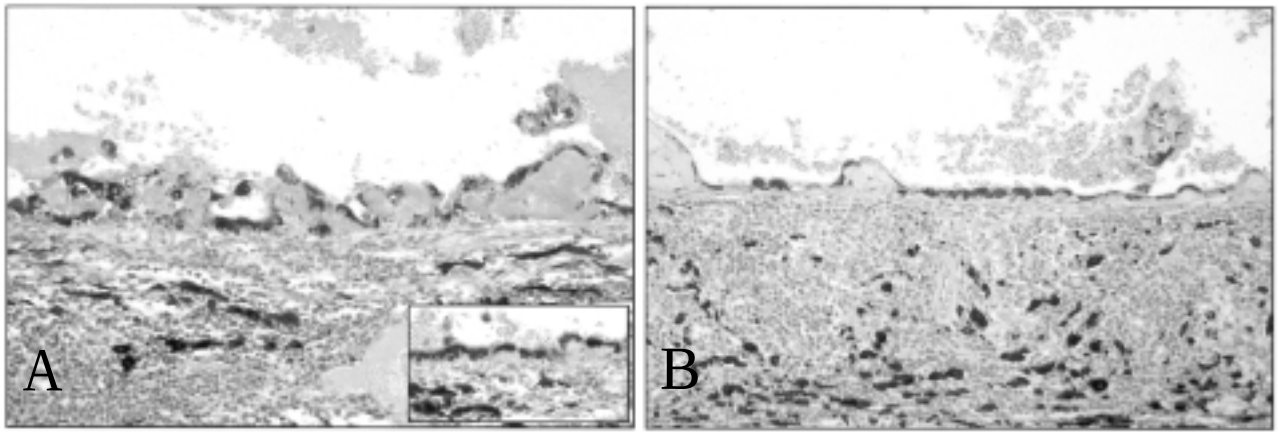

FIGURE 16

Immunohistochemical staining of posterior segment of eye with chronic uveitis for uPAR. A, RPE cells overlying Bruch's membrane demonstrate polarized immunoreactivity for uPAR along their basolateral membranes overlying chronic inflammatory infiltrate in choroid. Reaction product is also present in sub-RPE exudates between Bruch's membrane and the RPE cells. Weak positivity is also present in some leukocytes, endothelial cells, and stromal cells. Inset clearly demonstrates RPE immunoreactivity (hematoxylin counterstain, x200; inset, x1,000). B, Adjacent tissue section stained using idiotypic control antibody is negative (hematoxylin counterstain, x200).

(2) cleave plasminogen into fragments, which cannot be activated by uPA, thereby not only reducing uPA activation but also reducing the substrate upon which uPAR/uPA acts to produce proteolytic activity.[105] MMP-3 may also augment uPA/uPAR activity by its proteolytic activity of PAI-1, thereby impairing the inhibitory effect of vitronectin-bound PAI-1 and enhancing uPAR activity, which may alter cell adhesion and/or migration.[136]

The polarized expression of uPAR along the RPE basolateral membrane (Figures 3 and 16) may be due to its known association with other ligands and the cytoskeletal components, which has morphological and functional consequences. uPAR is known to closely associate with ß1 integrins in a symbiotic relationship in which they mutually regulate one another.[137] In the RPE, $ß_1$ integrins are known to be involved in the development and maintenance of polarity of the monolayer and are found along the apices and at the basolateral plasma membrane, where they are involved in adhesion to fibronectin, laminin, and collagen IV.[138] uPAR is a GPI-linked surface receptor that

requires association with other ligands to mediate its intracellular signaling.[139] Associations between uPAR and $ß_1$ integrins regulate uPAR distribution and, hence, its inability to generate concentrated proteolytic activity that overcomes its localized physiologic control due to PAI-1 inhibition.[73] Conversely, uPAR stabilizes the binding of $ß_1$ integrins to their ECM ligands[140] and so assists in maintaining RPE cell polarity and adhesion to Bruch's membrane. The analogous situation to this initially recognized in leukocytes was the association of uPAR with the $ß_2$ integrins, namely, CD11b/CD18 and CD11c/CD18.[139] In leukocytes, this association helps to control receptor expression and provides for intracellular uPAR signaling. However, when leukocytes become motile or are stimulated by LPS or proinflammatory cytokines, dissociation and capping of the receptors occur. For $ß_2$ integrins, capping mediates localized leukocyte adhesion to activated vascular endothelium or resident tissue cells, including RPE cells, expressing adhesion molecules, most notably intercellular adhesion molecule-1 (ICAM-1). For uPAR, capping at the leading edge of the motile cell subserves highly concentrated proteolysis to facilitate directed movement through the ECM.[103,141]

RPE cells are noteworthy with regard to uPAR expression, since they express $ß_1$, $ß_2$, and $ß_3$ integrins.[102,142,143] In so doing, the uPAR pattern of expression observed in this study suggests several consequences. First, the similar pattern of immunofluorescent staining observed for uPAR and CD11b in confluent cultures (Figure 4) and the extremely close proximity of these receptors as determined by RET of the fluorochromes labeling the receptors of rounded RPE cells (Figure 5) suggest that uPAR and CD11b/CD18 regulate the distribution and, hence, the biologic activity of one another. It is also likely that CD11b serves as the mediator for RPE uPAR, as it does in other cell types.[137] Dissociation of the two receptors results in homotypic aggregation and polarization of the RPE receptors, providing the polarized cells with a vanguard of proteolytic activity for ECM migration and aggregated CD11b to mediate RPE adhesion to other activated, ICAM-1–positive RPE cells as they burrow through the ECM or along surfaces coated with fibrin-rich exudates (Figure 16). The histopathologic patterns of RPE migration along subretinal neovascular membrane surfaces (Figures 13 and 14) and the strands of invading RPE cells seen in PVR membranes (Figure 15) argue for such a scenario.

The potential significance of uPAR $ß_1$ integrins is also suggested in the morphologic changes and RPE cell motility that were observed in each case as uPAR aggregated and migrated toward the lamellipodia of the RPE cells (Figure 5). Alterations in RPE polarity are known to be associated with changes in the distribution of $ß_1$ integrins, and uPAR is known to stabilize $ß_1$ integrin binding to their extracellular matrix ligands.[138] These facts, taken together with our observations, imply that the uPAR polarization witnessed in real time was associated with destabilization of $ß_1$ integrin contact points with the ECM, thereby allowing the RPE to detach from the matrix surface, polarize, and become motile (Figure 5), as later observed in the cell migration studies (Figures 11 and 12). Release of the RPE cells from attachment to their substrata, for example, is likely to permit them to migrate over the the tips of subretinal neovascular membranes as they emerge from the choroid into the subretinal space (Figures 13 and 14). RPE detachment due to release of $ß_1$ integrins is likely to have consequences besides loss of polarity. Among these are the binding of MMPs at sites of RPE $ß_1$ integrin evacuation from Bruch's membrane. The localized concentration of MMP activity and the enhanced uPAR/uPA activity on the nearby, capped RPE cell are likely to be synergistic in the ability to damage Bruch's membrane.

Another consequence of the loss of polarity is breakdown of the blood-retina barrier, which allows leakage of plasminogen and thrombin. The former is the substrate for elaboration of uPAR-generated proteolytic activity.[64] The latter[102] synergizes uPAR activity by inducing RPE uPAR gene transcription and cell surface expression. Thrombin also may activate pro–gelatinase A, which is constitutively secreted by vascular endothelial cells, monocytes, lymphocytes, and fibroblasts,[49,50] and is likely to be present at sites of blood-retina barrier breakdown. Activation of RPE-derived gelatinase A by the thrombin/activated protein C pathway may be particularly important in CNV, since high levels of thrombin have been shown in subretinal CNV lesions as well as in exudative sub-RPE lesions, which predispose to CNV.[51] Thrombin activation of RPE-derived gelatinase A would then result in proinflammatory cytokine-independent cleavage of collagen IV, since gelatinase A is not upregulated by TNF-γ or IL-1 or by uPAR-generated plasmin.[30] The results of this study strongly support this possibility, since RPE collagen IV lysis was not upregulated by IL-1 (Figure 7) while IL-1 stimulation of uPAR-dependent RPE proteolysis did occur (Figure 6). These results indicate that IL-1–generated RPE uPAR activity does not activate RPE pro–gelatinase A, which, therefore, relies on IL-1-independent triggers, such as thrombin, for its activation. The proinflammatory cytokine-independent cleavage of collagen IV by thrombin at sites of blood-retina barrier breakdown might then expose collagen I in the deeper layers of Bruch's membrane. Collagen I would then accelerate gelatinase A activation,[26] and consequently collagen IV lysis, by upregulating cell surface–associated MT1-MMP, which cleaves pro–gelatinase A into its active form.[26] The

gelatinase A mechanisms of collagen IV lysis in the ECM of Bruch's membrane or PVR membranes are not likely to be modulated by therapy aimed at inhibition of proinflammatory cytokines such as IL-1 or TNF.

This is the first study to show actual cleavage of native interstitial collagen and elastin by secreted RPE MMPs. The importance of this finding is reflected in the composition of the ECM comprising Bruch's membrane and PVR membranes. Bruch's membrane is a multilayered structure composed of basement membranes of the RPE and endothelium of the choriocapillaris sandwiching central lamellae containing structural collagens and elastin, which are enmeshed in proteoglycans and glycosaminoglycans.[144] The basement membranes are rich in collagen IV, fibronectin, and laminin. The collagenous layers are composed principally of collagens I and III, while the central elastic layer is composed chiefly of elastin.[4] Exposure of the collagenous layers and central elastic layer deep in Bruch's membrane makes it subject to the effects of interstitial collagenase (collagenase 1; MMP-1) and elastase, both of which are secreted by cells, including RPE cells constitutively (Figures 8 and 9). MMP-1, secreted as a latent procollagenase 1, requires enzymatic cleavage for its activation. In vivo activation may occur by previously activated uPAR or MMP.

RPE secretion of collagenase and elastase, together with that generated by the choriocapillaris vascular endothelium, may be important to physiologic remodeling of Bruch's membrane.[145,146] These MMPs are almost certainly tightly regulated by TIMPs whose impairment may lead to progressive alterations. It is known that genetic alterations of TIMP-3 lead to premature severe RPE and Bruch's membrane alterations that may be due to unbridled MMP activity. Reduced RPE TIMP-3 expression also results from RPE exposure to near-ultraviolet light,[147] a relative risk factor for the development of ARMD. Routinely, progressive alterations in Bruch's membrane in human eyes begin in the third decade of life.[148,149] These include abnormal RPE basement membrane thickening due in large measure to RPE extrusion of undigested lipid, protein, and lysosomal debris into Bruch's membrane.[148,150-153] In eyes predisposed to ARMD, MMP-1 may also be activated by lysosomal enzymes, which are secreted directly by aging and/or dysfunctional RPE cells into Bruch's membrane in secondary lysosomes.[154-158] Once activated, collagenase cleaves within the triple helical domains of tropocollagen near the carboxyl terminus, resulting in one-quarter and three-quarter chain length fragments that are susceptible to further digestion by other proteolytic enzymes, including TIMPs and lysosomal enzymes.[159-161] Since MMP-1 hydrolyzes interstitial collagen types I, II, and III,[160,161] it is likely to be important in generating full-thickness defects in Bruch's membrane that permit subretinal CNV to occur. MMP-1 might also participate in remodeling and RPE invasion into PVR membranes which have been shown to be composed principally of collagens I, II, and III. Elastase is an MMP and a neutral endopeptidase, which not only hydrolyzes elastin but also cleaves other proteins, including proteinase inhibitors, thereby potentiating the hydrolytic activities of the MMPs.[162-164]

In this study, the IL-1 upregulation of secreted RPE interstitial collagenase (Figure 8) and elastase (Figure 9) that hydrolyzed their native substrates indicates that this may actually occur in retinal lesions of CNV and PVR in which RPE cells, mononuclear phagocytes, vascular endothelial cells, and other cells known to generate ambient IL-1 are present. Devitalized RPE cells or RPE cells involved in reparative responses may release inappropriately high levels of MMPs. In addition to ambient proinflammatory cytokines, phagocytosis of particulate debris and growth factors may induce the RPE to secrete excessive levels of collagenase and elastase, leading to the Bruch's membrane defects which predispose to CNV.

This study also demonstrates for the first time that RPE uPAR may be upregulated by several proinflammatory cytokines known to be elaborated in retinal lesions (Figures 1, 2, and 6). TNF, as well as IL-1, is elaborated by leukocytes, vascular endothelial cells, and RPE cells. These mediators stimulate RPE cells to express cell surface receptors and secrete chemokines, most notably IL-8 and MCP-1, which recruit and activate the leukocytes perpetuating the inflammatory components of CNV, PVR, and uveitic lesions. Thrombin, known to potentiate these RPE inflammatory responses, is an important initiator of MMP-2 and uPAR/uPA proteolytic activity.[26] That such proinflammatory cytokine upregulation of uPAR actually occurs in vivo is confirmed by the polarized, enhanced induction of uPAR that was observed over the inflammatory choroidal uveitic infiltrates, particularly in regions where sub-RPE exudates, rich in plasma-derived proteins including thrombin, were present (Figure 16).

Low-grade inflammation is associated with the development of CNV.[165-167] Approximately 60% of surgically excised, active CNV membranes contain mononuclear phagocytes, regardless of the underlying disease.[8-12] Mononuclear phagocytes specifically have been associated with normal retinal vasculogenesis during development and in reparative and pathologic angiogenesis, in which they release factors that influence various phases of the angiogenic process.[168,169] These growth factors, aFGF, bFGF, TGF-ß, and vascular endothelial growth factor (VEGF), all of which have been identified in surgically excised CNV,[170,171] and TNF-α may stimulate RPE expression of VEGF[172,173] and chemokines IL-8 and MCP-1, the former an inducer of angiogenesis and the latter a prime

recruiter and activator of mononuclear phagocytes.[174,175]

uPA, uPAR, and PAI-1 are also observed during angiogenesis in vivo where they are found to be expressed by the proliferating vascular endothelial cells. In this study, uPAR expression was found on human RPE cells as well as on the vascular endothelium of CNV membranes (Figures 13 and 14). VEGF and bFGF increase uPA and uPAR in cultured vascular endothelial cells. Induction of uPAR is accompanied by a decreased affinity for uPA and concomitant induction of PAI-1, but the overall effect is to favor proteolysis.[176] TGF-ß, an inducer of RPE uPAR,[88] acts as a pleotropic cytokine, having both negative and positive effects on endothelial proteolytic activity by inducing both uPA and PAI-1, with an overall effect favoring PAI-1 inhibition of proteolysis.

A recent study by Davis and associates[177] illustrates the careful regulation of angiogenesis by coordinated activity of uPAR/uPA, interstitial collagenase (MMP-1), and gelatinase B, all of which are produced by the RPE and, as shown in this study (Figures 2, 6, and 8), all of which are increased by IL-1.[59] These investigators found unencumbered MMP-1 and MMP-9 activation by uPAR-induced activation of plasminogen-induced vascular endothelial cell apoptosis and capillary regression that was apparently due to overexuberant ECM digestion. Accordingly, TIMPs and PAI-1 both blocked capillary regression, while antibodies to PAI-1 accelerated it. Thus, for neovascularization, uPAR/uPA and its inhibitor, PAI-1, and MMPs and their inhibitors, TIMPs, require careful coordination so as to provide the proper degree of ECM proteolysis for new blood vessels to proliferate.

uPAR also specifically interacts with the $ß_3$ integrin, $\alpha_v ß_3$, the major vitronectin receptor that is expressed by many cell types, including macrophages,[178] vascular endothelial cells,[179] epithelial cells,[180] smooth-muscle cells,[181] and cancer cells, including melanoma.[182] $\alpha_v ß_3$ is associated with cellular migration, ECM proteolysis, angiogenesis, and metastasis. Ligation of $\alpha_v ß_3$ with mAb increases gene expression of uPAR and PAI-1 mRNA and cell-surface plasmin, resulting in increased cell invasion of collagen gels that can be abolished by mAb to uPA and uPAR.[183] Vitronectin binding to uPAR inhibits $ß_1$ integrin–mediated attachment to ECM and $ß_2$ integrin (CD11b/CD18)–mediated phagocytosis of fibrinogen.[184] $ß_1$ integrin–mediated attachment to vitronectin also appears to be uPAR-dependent.[140]

In melanoma, vitronectin is a marker of malignant progression and has been implicated in apoptosis[185] and production of MMP-2.[186] Melanoma cell migration on a vitronectin matrix is inhibited by uPA, whereas PAI-1 promoted melanoma cell migration on vitronectin, supporting the concept that uPA/uPAR acts as a vitronectin receptor that plays a role in regulating cell migration and adhesion.[187] uPA/uPAR complex can bind to vitronectin either indirectly through the vitronectin-associated PAI-1 or directly through specific uPAR domains.[188]

In this study, the relative contributions of uPAR and MMPs to the process of RPE migration were investigated using a novel collagen gel supported by nylon mesh to prove the hypothesis that RPE uPAR mediated activation of proteolysis mediates RPE migration through ECM. As with angiogenesis, the uPAR/uPA and MMPs are both likely to be operative. However, the relative importance of these agents to pericellular proteolysis, the key step required for the invasion of cells through basement membranes and interstitial tissues, varies among cell types[124,189-196] and is unknown in the RPE cells. Pericellular proteolysis due to RPE uPAR activity (Figure 6) and RPE MMP activity (Figure 7) was initially confirmed by placing the RPE cells on gels containing Bodipy-BSA (albumin) and DQ collagen (collagen IV) probes, respectively. Pericellular fluorescence due to matrix disruption and probe hydrolysis that generated fluorescent products indicated constitutive RPE expression of both activities. Disruption of matrices in the presence of the inhibitors PAI-1 and 1,10-phenanthroline substantially inhibited the release of fluorescent peptides from Bodipy-BSA and DQ collagen, respectively, demonstrating that the enzymatic activities were specific ($P<.001$). IL-1 enhanced PAI-1-inhibitable, specific activity of RPE uPAR ($P<.001$), but not of collagen IV MMP-hydrolytic activity, a finding consistent with the lack of induction of gelatinase by IL-1.[30]

To demonstrate the relative importance of uPAR and MMP in actual RPE migration, however, a novel transmigration assay system to prove the hypothesis of this thesis was developed (Figure 10).[133] The transmigration assay method is of considerable interest from both technologic and physiologic viewpoints. Using an open-mesh nylon grid for support, multiple gel layers were deposited on the mesh. By adding a small amount of gel to the mesh at a time, multiple layers could be built up into a thicker matrix, much like assembling plywood. The open mesh also affords the ability to use both transmitted light and epifluorescence microscopy to image events. This has considerable advantage over invasion assays that rely on cell migration through artificial pores. Another advantage of these nylon mesh–supported matrices is that most of the surface area is available for transmigration to the bottom of the matrix. In contrast, only a small fraction of a conventional filter's surface area is available in the form of small pores to permit migration to the bottom of the matrix. In most experiments using filter assays, cells must deform as they pass through the artificial matrix pores, an action event that has no clear counterpart in cell physiology. Moreover, pore assays may be measuring the abilities of cells to find an available pore rather than the kinetics of

transmigration. A clear advantage of these gel matrices is that they can also be tailored to address specific experimental hypotheses, such as the one in this study. In this study, for example, we included substrates (Bodipy-BSA and DQ collagen) within the matrix that become fluorescent upon proteolytic cleavage, thus revealing the location of functioning enzymes while imaging transmigrating red, fluorescently labeled RPE cells. When these assays were conducted for extended periods of time, the pathways followed by cells during this model transmigration process could be imaged. Our approach is particularly valuable in studying transmigration, since bright-field microscopy is unrevealing under these circumstances because the refractive index of cells matches that of the ECM. Thus, we have developed the technology suitable for addressing several critical issues surrounding the invasive ability of cells.

To demonstrate RPE migration, the novel nylon mesh–supported collagen gels were seeded with RPE cells (Figure 10) and induced to migrate with serum. Imaging of the migrating RPE cells over 4 hours revealed plumes of fluorescence generated by the RPE cells as they tunneled through the matrix (Figure 11). To confirm the relevance of uPAR and MMP activities to the transmigration of RPE cells through the novel matrices, PAI-1 and 1,10-phenanthroline were incorporated into the matrices at high concentrations before their solidification. PAI-1, but not 1,10-phenanthroline, was found to substantially inhibit ($P<.001$) the ability of RPE cells to cross the matrix (Figure 12). This dramatic difference is strong evidence for a cardinal role for uPAR in RPE migration through ECM.

Studies of other cell types, including cancer cells, have shown that uPAR-positive cells are more invasive.[195-199] However, uPAR-negative cells can also be invasive, since the presence of uPAR-positive cells may enhance the ability of uPAR-negative cells to migrate across the ECM. Microscopy studies suggest that the ability of uPAR-negative cells to follow uPAR-positive cells across a matrix can partially account for this.[133] Having developed the technology to observe proteolytic trails in matrices, we examined the process of RPE invasion and found that trailing RPE cells used the paths of matrix disruption by the initial migrants, facilitating their passage. Such a process in vivo might allow a relatively few strongly expressing uPAR-positive RPE cells to pave the way for others to follow, resulting in the strands and other cellular arrangements usually seen in histopathologic sections of CNV and PVR membranes (Figures 13, 14, and 15).

In this scenario, uPAR clustering at RPE cell–substratum interfaces and at migratory fronts[200-203] would render the ECM susceptible to digestion by cell-associated plasmin that is activated by uPA bound to RPE uPAR. RPE uPAR, found at the lamellipodium of elongated RPE cells in areas of blood-retina barrier breakdown, RPE cell disruption, or persistent retinal detachment, would then have focused proteolytic action in the direction of cell migration. Plasmin degradation, potentiated and controlled to some degree by the MMPs/TIMPs, would degrade ECM proteins in the path of cellular invasion.[204] This scenario is now a working hypothesis for current research and development of drugs to prevent cancer cell invasion and metastasis. Understanding the roles of uPAR and MMP in RPE migration may lead to the development of new pharmacologic agents targeting uPAR participation in adverse pathophysiologic mechanisms of important retinal diseases.

ACKNOWLEDGMENTS

Special thanks to Victor M. Elner, MD, PhD, Howard R. Petty, PhD, Andrei L. Kindzelskii, MD, Ersalan Rahman, MD, and Mitch Gillett for their expertise and contributions in data acquisition, tissue preparation, and manuscript preparation.

REFERENCES

1. Bressler NM, Bressler SB, Fine SL. Age-related macular degeneration. *Surv Ophthalmol* 1988;32:375-413.
2. Green WR, Enger C. Age related macular degeneration histopathological studies. *Ophthalmology* 1993;100:1519-1535.
3. Hogan MJ. Role of the retinal pigment epithelium in macular disease. *Trans Am Acad Ophthalmol Otolaryngol* 1972;76:64-80.
4. Feeney-Burns L, Ellersieck M. Age-related changes in the ultrastructure of Bruch's membrane. *Am J Ophthalmol* 1985;100:686-697.
5. Green WR. The retina. In: Spencer WH, ed. *Ophthalmic Pathology. An Atlas and Textbook*. Philadelphia: WB Saunders; 1996: 982-1050.
6. Green WR, Key SN III. Senile macular degeneration. A histopathologic study. *Trans Am Ophthalmol Soc* 1977;75:951-955.
7. Green WR. Clinicopathologic studies of treated choroidal neovascular membranes. A review and report of two cases. *Retina* 1991;11:328-356.
8. Lopez PF, Grossniklaus HE, Lambert HM, et al. Pathologic features of surgically excised subretinal neovascular membranes in age-related macular degeneration. *Am J Ophthalmol* 1991;112:647-656.
9. Saxe SJ, Grossniklaus HE, Lopez PF, et al. Ultrastructural features of surgically excised subretinal neovascular membranes in the ocular histoplasmosis syndrome. *Arch Ophthalmol* 1993;111:88-95.
10. Grossniklaus HE, Martinez JA, Brown VE, et al. Immunohistochemical and histochemical properties of surgically excised subretinal neovascular membranes in age-related macular degeneration. *Am J Ophthalmol* 1992;114:464-472.
11. Grossniklaus HE, Hutchinson AK, Capone A Jr, et al. Clinicopathologic features of surgically excised choroidal neovascular membranes. *Ophthalmology* 1994;101:1099-1111.
12. Grossniklaus HE, Green WR. Histopathologic and ultrastructural findings of surgically excised choroidal neovascularization. *Arch Ophthalmol* 1998;116:745-749.

13. Weber BHF, Vogt G, Wolz W, et al. Sorsby's fundus dystrophy is genetically linked to chromosome 22q13-qter. *Nature Genet* 1994;7:158-161.
14. Matrisian LM. Metalloproteinases and their inhibitors in matrix remodeling. *Trends Genet* 1990;6:121-125.
15. Weber BHF, Vogt G, Pruett RC, et al. Mutations in the tissue inhibitor of metalloproteinases-3 (TIMP3) in patients with Sorsby's fundus dystrophy. *Nature Genet* 1994;8:352-356.
16. Capon MRC, Marshall J, Krafft JI, et al. Sorsby's fundus dystrophy – A light and electron microscopic study. *Ophthalmology* 1989;96:1769-1777.
17. Fariss RN, Apte SS, Luthert PJ, et al. Accumulation of tissue inhibitor of metalloproteinases-3 in human eyes with Sorsby's fundus dystrophy or retinitis pigmentosa. *Br J Ophthalmol* 1998;82:1329-1334.
18. Kamei M, Hollyfield JG. TIMP-3 in Bruch's membrane: changes during aging and in age-related macular degeneration. *Invest Ophthalmol Vis Sci* 1999;40:2367-2375.
19. Bressler SB, Bressler NM, Alexander J, et al. Clinicopathologic correlation of occult choroidal neovascularization in age-related macular degeneration. *Arch Ophthalmol* 1992;110:827-832.
20. Gass DM. Drusen and disciform macular detachment and degeneration. *Arch Ophthalmol* 1973;90:201-217.
21. Green WR, Key SN. Pathologic features of senile macular degeneration. *Ophthalmology* 1985;92:615-627.
22. Sarks SH. Aging and degeneration in the macular region: a clinicopathologic study. *Br J Ophthalmol* 1976;60:324-341.
23. Smiddy WE, Fine SL. Prognosis of patients with bilateral macular drusen. *Ophthalmology* 1984;91:271-284.
24. Wright JK, Cawston TE, Hazleman BL. Transforming growth factor beta stimulates the production of the tissue inhibitor of metalloproteinases (TIMP) by human synovial and skin fibroblasts. *Biochim Biophys Acta* 1991;1094:207-210.
25. Stetler S. Matrix metalloproteinases in angiogenesis: a moving target for therapeutic invervention. *J Clin Invest* 1999;103:1237-1241.
26. Nguyen M, Arkell J, Jackson CJ. Human endothelial gelatinases and angiogenesis. *Int J Biochem Cell Biol* 2001;33:960-970.
27. Butler TA, Zhu C, Mueller RA, et al. Inhibition of ovulation in the perfused rat ovary by the synthetic collagenase inhibitor SC 44463. *Biol Reprod* 1991;44:1183-1188.
28. Grahan CH, Lala PK. Mechanism of control trophoblast invasion in situ. *J Cell Phys* 1991;148:228-234.
29. Ye S. Polymorphism in matrix metalloproteinase gene promoters: implication in regulation of gene expresion and susceptibility of various diseases. *Matrix Biol* 2000;19:623-629.
30. Jackson C, Nguyen M, Arkell J, et al. Selective matrix metalloproteinase (MMP) inhibition in rheumatoid arthritis—targetting gelatinase A activation. *Inflamm Res* 2001;50:183-186.
31. Zucker S, Lysik RM, Zarrabi MH, et al. Elevated plasma stromelysin levels in arthritis. *J Rheumatol* 1991;21:2329-2333.
32. Naito K, Takahashi M, Kushida K, et al. Measurement of matrix metalloproteinases (MMPs) and tissue inhibitor of metaloproteinases-1 (TIMP-1) in patients with knee osteoarthritis; comparison with generalized osteoarthritis. *Rheumatology* (Oxford) 1999;38:510-515.
33. Liotta L, Steeg PS, Stetler Stevenson WG. Cancer metastasis and angiogenesis: an imbalance of positive and negative regulation. *Cell* 1991;327-336.
34. McCawley LJ, Matrisian LM. Tumor progression:defining the soil round the tumor seed. *Curr Biol* 2001;11:R25-R27.
35. McMillan WD, Pearce WH. Increased plasma levels of metalloproteinase-9 are associated with abdominal aortic aneurysms. *J Vasc Surg* 1999;29:122-127.
36. Kai H, Ikeda H, Yasukawa H, et al. Peripheral blood levels of matrix metalloproteases-2 and -9 are elevated in patients with acute coronary syndromes. *J Am Coll Cardiol* 1998;32:368-372.
37. Henney AM, Wakeley PR, Davies MJ, et al. Localization of stromelysin gene expression in atherosclerotic plaques by in situ hybridization. *Proc Natl Acad Sci USA* 1991;88:8154-8158.
38. Galis ZS, Sukhova GK, Lark MW, et al. Increased expression of matrix metalloproteinases and matrix degrading activity in vulnerable regions of human atherosclerotic plaques. *J Clin Invest* 1994;94:2493-2503.
39. Kleiner DE, Stetler Stevenson WG. Matrix metalloproteinases and metastasis. (Abstract) *Cancer Chemo Pharmacol* 1999;43(Suppl):S42-S51.
41. Brinckerhoff CE, Rutter JL, Benbow U. Interstitial collagenases as markers of tumor progression. *Clin Cancer Res* 2000;6:4823-4830.
40. Nagase H, Woessner JF, Jr. Matrix metalloproteinases. *J Biol Chem* 1999;274:21491-21492.
42. Murray GI, Duncan ME, O'Neil P, et al. Matrix metalloproteinase-1 is associated with poor prognosis in colorectal cancer. *Nat Med* 1996;2:461-462.
43. Murray GI, Duncan ME, O'Neil P, et al. Matrix metalloproteinase-1 is associated with poor prognosis in oesophageal cancer. *J Pathol* 1998;185:256-261.
44. Ito T, Ito M, Shiozawa J, et al. Expression of the MMP-1 in human pancreatic carcinoma: relationship with prognostic factor. *Mod Pathol* 1999;12:669-675.
45. Walsh DA. Angiogenesis and arthritis. *Rheumatology* 1999;38:103-12.
46. Frisch SM, Morasaki JH. Positive and negative transcriptional elements of the human type IV collagenase gene. *Mol Biol Cell* 1990;10:6524-6532.
47. Olson MW, Gervasi DC, Mobashery S, et al. Kinetic analysis of the binding of human matrix metalloproteinase-2 and -9 to tissue inhibitor of metalloproteinase TIMP-1 and TIMP-2. *J Biol Chem* 1977;272:29975-29983.
48. Howard E, Bulleten E, Banda MJ. Regulation of the autoactivation of human 72kDa progelatinase by tissue inhibitor of metalloproteinase-2. *J Biol Chem* 1991;266:13064-13069.
49. Jackson CJ, Arkell J, Nguyen M. Rheumatoid synovial endothelial cells secrete decreased levels of tissue inhibitor of MMP (TIMP1). *Ann Rheum Dis* 1998;57:158-161.
50. Opdenakker G, Van den Steen PE, Dubois B, et al. Gelatinase B functions as regulator and effector in leukocyte biology. *J Leukoc Biol* 2002;69:851-859.
51. Fenton JW. Regulation of thrombin generation and functions. *Semin Thromb Hemost* 1988;14:234-239.
52. Nguyen M, Arkell J, Jackson CJ. Active and tissue inhibitor of matrix metalloproteinase-free gelatinase B accumulates within human microvascular endothelial vesicles. *J Biol Chem* 1998;273:5400-5404.
53. Opdenakker G, Masure S, Grillet B, et al. Cytokine-mediated regulation of human leukocyte gelatinases and role in arthritis. *Lymphokine Cytokine Res* 1991;10:317-324.
54. Gijbels K, Masure S, Carton H, et al. Gelatinase in the cerebrospinal fluid of patients with multiple sclerosis and other inflammatory neurological disorders. *J Neuroimmunol* 1992;41:29-34.
55. Schonbeck U, Mach F, Libby P. Generation of biologically active IL-1ß by matrix metalloproteinases: a novel caspase-1-independent pathway of IL-1ß processing. *J Immunol* 1998;161:3340-3346.

56. McQuibban GA, Gong J-H, Tam EM, et al. Inflammation dampened by gelatinase A cleavage of monocyte chemoattractant protein-3. *Science* 200;289:1202-1206.
57. Nagase H. Stromelysins 1 and 2. In: Parks WC, Mecham RP, eds. *Matrix Metalloproteinases*. San Diego: Academic Press; 1998:43-84.
58. Newman KM, Ogata Y, Malon AM, et al. Identification of matrix metalloproteinases 3 (stromelysin-1) and 9 (gelatinase B) in abdominal aortic aneurysm. *Arterioscler Thromb* 1994;14:1315-1320.
59. Alexander JP, Bradley JMB, Gabourel JD, et al. Expression of matrix metalloproteinases and inhibitor by human retinal pigment epithelium. *Invest Ophthalmol Vis Sci* 1990;31:2520-2528.
60. Schonfeld CL. Metalloproteinase stromelysin. Expression in humanem retinalem pigmentepithel (RPE). *Ophthalmologe* 1997;94:629-633.
61. Hunt RC, Fox A, Pakalnis VA, et al. Cytokines cause cultured retinal pigment epithelial cells to secrete metalloproteinases and to contract collagen gels. *Invest Ophthalmol Vis Sci* 1993;34:3179-3186.
62. Vaisanen A, Kallioinen M, Von Dickhoff K, et al. Matrix metalloproteinase-2 (MMP-2) immunoreactive protein—a new prognostic marker in uveal melanoma. *J Pathol* 1999;188:56-62.
63. Ruiz A, Brett P, Bok D. TIMP-3 is expressed in the human retinal pigment epithelium. *Biochem Biophys Res Comm* 1996;226:467-474.
64. Andreasen PA, Kjoller L, Christensen L, et al. The urokinase-type plasminogen activator system in cancer metastasis: a review. *Int J Cancer* 1997;72:1-22.
65. Ploug M, Ronne E, Behrendt N, et al. Cellular receptor for urokinase plaminogen activator. Carboxyl-terminal processing and membrane anchoring by glycosyl-phosphatidyl-inositol. *J Biol Chem* 1991;266:1926-1933.
66. Stoppelli MP, Corti A, Soffientini A, et al. Differentiation-enhanced binding of the amino-teminal fragment of human urokinase plasminogen activator to a specific receptor on U937 monocytes. *Proc Natl Acad Sci USA* 1985;82:4939-4943.
67. Dano K, Behrendt N, Brenner N, et al. The urokinase receptor. Protein structure and role in plasminogen activation and cancer invasion. *Fibrinolysis* 1994;8:189-203.
68. Plesner T, Ploug M, Ellis V, et al. The receptor for urokinase-type plasminogen activator and urokinase is translocated from two distinct intracellular compartments to the plasma membrane on stimulation of human neutrophils. *Blood* 1994;83:808-815.
69. McNeill H, Jensen PJ. A high-affinity receptor for urokinase plasminogen activator on human keratinocytes: characterization and potential modulation during migration. *Cell Regul* 1990;1:843-852.
70. Miles LA, Levin EG, Plescia J, et al. Plasminogen receptors, urokinase receptors, and their modulation on human endothelial cells. *Blood* 1988;72:628-635.
71. Hollas W, Hoosein N, Chung W, et al. Expression of urokinase and its receptor in invasive and non-invasive prostate cancer cell lines. *Thromb Haemost* 1992;68:662-666.
72. Boyd D, Florent H, Kin P, et al. Determination of the levels of urokinase and its receptor in human colon carcinoma cell lines. *Cancer Res* 1988;48:3112-3116.
73. Ghosh S, Brown R, Jones JC, et al. Urinary-type plasminogen activator (uPA) expression and uPA receptor localization are regulated by alpha 3 beta 1 integrin in oral keratinocytes. *J Biol Chem* 2000;275:23869-23876.
74. Kessler TL, Markus G. Epidermal growth factor and 12-tetradecanoyl phorbol 13-acetate induction of urokinase in A431 cells. *Semin Thromb Hemost* 1991;17:217-224.
75. Mignatti P, Mazzieri R, Rifkin DB. Expression of the urokinase receptor in vascular endothelial cells is stimulated by basic fibroblast growth factor. *J Cell Biol* 1991;113:1193-1201.
76. Lund LR, Romer J, Ronne E, et al. Urokinase-receptor biosynthesis, mRNA level and gene transcription are increased by transforming growth factor beta 1 in human A549 lung carcinoma cells. *EMBO J* 1991;10:3399-3407.
77. Neidbala MJ, Stein M. Tumor necrosis factor induction of urokinase-type plasminogen activator in human endothelial cells. *Biomed Biochim Acta* 1991;50:427-436.
78. Ellis V, Scully MF, Kakkar VV. Plasminogen activation initiated by single chain urokinase-type plasminogen activator. Potentiation by U937 monocytes. *J Biol Chem* 1989;264:2185-2188.
79. Olson D, Pollanen J, Hoyer-Hansen G, et al. Internalization of the urokinase-plasminogen activator type-1 complex is mediated by the urokinase receptor. *J Biol Chem* 1992;267:9129-9133.
80. Kircheimer JC, Christ G, Binder BR. Growth stimulation of human epidermal cells by urokinase is restricted to the intact active enzyme. *Eur J Biochem* 1989;181:103-107.
81. Odekon LE, Sato Y, Rifkin DB. Urokinase-type plasminogen activator mediates basic fibroblast growth factor-induced bovine endothelial cell migration independent of its proteolytic activity. *J Cell Physiol* 1992;150:258-263.
82. Gyetko MR, Sitrin RG, Fuller JA, et al. Function receptor (CD87) in neutrophil chemotaxis. *J Leukoc Biol* 1995;58:533-538.
83. Tripathi RC, Tripathi BJ, Park JK. Localization of urokinase-type plasminogen activator in human eyes: an immunocytochemical study. *Exp Eye Res* 1990;51:545-552.
84. Siren V, Stephens RW, Salonen EM, et al. Retinal pigment epithelial cells secrete urokinase-type plasminogen activator and its inhibitor PAI-1. *Ophthalmic Res* 1992;24:203-212.
85. Campochiaro PA, Mimuro J, Sugg R, et al. Retinal pigment epithelial cells produce a latent fibrinolytic inhibitor that is antigenically and biochemically related to type 1 plasminogen activator inhibitor produced by vascular endothelial cells. *Exp Eye Res* 1989;49:195-203.
86. Siren V, Immonen I, Cantell K, et al. Interferons a and g inhibit plasminogen activator inhibitor-1 gene expression in human retinal pigment epithelial cells. *Ophthalmic Res* 1994;25:1-7.
87. Yang Z, Cohen RL, Lui GM, et al. Thrombin increases expression of urokinase receptor by activation of the thrombin receptor. *Invest Ophthalmol Vis Sci* 1995;36:2254-2261.
88. Siren V, Myohanen H, Vaheri A, et al. Transforming growth factor beta induces urokinase receptor expression in cultures retinal pigment epithelial cells. *Ophthalmic Res* 1999;31:184-191.
89. Jerdan JA, Pepose JS, Michels RG, et al. Proliferative vitreoretinopathy membranes. An immunohistochemical study. *Ophthalmology* 1989;96:801-810.
90. Marino I, Hiscott P, McKechnie N, et al. Variation in epiretinal membrane components with clinical derivation of the proliferative tissue. *Br J Ophthalmol* 1990;74:393-399.
91. Kauffmann DJH, van Meurs JC, Mertens DAE, et al. Cytokines in vitreous humor: interleukin-6 is elevated in proliferative vitreoretinopathy. *Invest Ophthalmol Vis Sci* 1994;35:900-906.
92. Elner SG, Elner VM, Jaffe GJ, et al. Cytokines in proliferative diabetic retinopathy and proliferative vitreoretinopathy. *Curr Eye Res* 1995;14:1045-1053.
93. Limb GA, Earley AO, Green W, et al. Distribution of cytokine proteins within epiretinal membranes in proliferative vitreoretinopathy. *Curr Eye Res* 1994;13:791-798.

94. Grant MB, Guay C, Marsh R. Insulin-like growth factor 1 stimulates proliferation, migration, and plasminogen activator release by human retinal pigment epithelial cells. *Curr Eye Res* 1990;9:323-335.
95. Reuning U, Magdolen V, Wilhelm O, et al. Multifunctional potential of the plasminogen activation system in tumor invasion and metastasis (review). *Int J Oncol* 1998;13:893-906.
96. Blasi F. uPA, uPAR, PAI-1: key intersection of proteolytic, adhesive, and chemotactic highways? *Immunol Today* 1997;18:415-417.
97. Fibbi G, Ziche M, Morbidelli L, et al. Interaction of urokinase with specific receptors stimulates mobilization of bovine adrenal capillary endothelial cells. *Exp Cell Res* 1988;179:385-395.
98. Gudewicz PW, Bilboa N. Human urokinase-type plasminogen activator stimulates chemotaxis of human neutophils. *Biochem Biophys Res Comm* 1987;147:1176-1181.
99. Resnati M, Guttinger M, Valcamonica S, et al. Proteolytic cleavage of the urokinase receptor substitutes for the agonist-induced chemotactic effect. *EMBO J* 1996;15:1572-1582.
100. Loskutoff DJ, Curriden SA, Hu G, et al. Regulation of cell adhesion by PAI-1. *APMIS* 1999;107:54-61.
101. Elner VM, Schaffner T, Taylor K, et al. Immunophagocytic properties of retinal pigment epithelium cells. *Science* 1982; 211:74-76.
102. Pavilack MA, Elner SG, Feldman LE, et al. Human RPE cells express leukocyte integrins and intercellular adhesion molecules. (Abstract) *Invest Ophthalmol Vis Sci* 1990;31(Suppl):372. Abstract 1828.
103. Xue W, Kindzelskii AL, Todd III RF, et al. Physical association of complement receptor type 3 and urokinase-type plasminogen activator receptor in neutrophil membranes. *J Immunol* 1994;152:4630-4640.
104. Arribas J, Coodly L, Vollmer P, et al. Diverse cell surface protein ectodomains are shed by a system sensitive to metalloprotease inhibitors. *J Biol Chem* 1996;271:11376-11382.
105. Lijnen HR. Elements of the fibrinolytic system. *Ann NY Acad Sci* 2001;936:226-236.
106. Koolwijk P, Sidenius N, Peters E, et al. Proteolysis of the urokinase-type plasminogen activator receptor by metalloproteinase-12; implication for angiogenesis in fibrin matrices. *Blood* 2001;97:3123-3131.
107. Okamoto I, Kawano Y, Tsuiki H, et al. CD44 cleavage induced by a membrane associated metalloprotease plays a critical role in tumor cell migration. *Oncogene* 1999;18:1435-1446.
108. Preece G, Murphy G, Ager A. Metalloproteinase-mediated regulation of L-selectin levels on leucocytes. *J Biol Chem* 1996;271:11645-11640.
109. Elner SG, Strieter RM, Elner VM, et al. Monocyte chemotactic protein gene expression by cytokine-treated human retinal pigment epithelial cells. *Lab Invest* 1991;64:819-825.
110. Campochiaro PA, Jerdon JA, Glaser BM. The extracellular matrix of human retinal pigment epithelial cells in vivo and its synthesis in vitro. *Invest Ophthalmol Vis Sci* 1986;27:1615-1621.
111. Bohuslav J, Horejsi V, Hansmann C, et al. Urokinase plasminogen activator receptor, ß$_2$-integrins, and *src*-kinases within a single receptor complex of human monocytes. *J Exp Med* 1995;181:1381-1390.
112. Min HY, Semnani R, Mizukami IF, et al. cDNA for Mo3, a monocyte activation antigen, encodes the human receptor for urokinase plasminogen activator. *J Immunol* 1992;148:3636-3642.
113. Todd RF, Nadler LM, Schlossman SF. Antigens on human monocytes identified by monoclonal antibodies. *J Immunol* 1981;126:1435-1442.
114. Todd RF, Roach JA, Arnaout MA. The modulated expression of Mo5, a human myelomonocyte plasma membrane antigen. *Blood* 1985;65:964-973.
115. Dana N, Styrt B, Griffin JD, et al. Two functional domains in the phagocyte membrane glycoprotein Mo1 identified with monoclonal antibodies. *J Immunol* 1986;137:3259-3263.
116. Petty HR, Francis JW, Todd RF, et al. Neutrophil C3bi receptors: formation of membrane clusters during cell triggering requires intracellular granules. *J Cell Physiol* 1987;133:235-242.
117. Zhou MJ, Todd RF, Petty HR. Detection of transmembrane linkages between immunoglobulin or complement receptors and the neutrophil's cortical microfilaments by resonance energy transfer microscopy. *J Mol Biol* 1991;218:263-268.
118. Zhou MJ, Todd RF III, van de Winkel JG, et al. Cocapping of the leukoadhesion molecules complement receptor type 3 and lymphocyte function-associated antigen-1 with Fcg receptor III on human neutrophils: possible role of lectin-like interactions. *J Immunol* 1993;150:3030-3041.
119. Wessendorf MW, Appel NM, Elde R. Simultaneous observation of fluorescent retrogradely labeled neurons and the immunofluorescently labeled fibers apposing them using fluoro-gold and antisera labeled with the blue fluorochrome7-amino-4-methylcoumarin-3-acetic acid (AMCA). *Neurosci Lett* 1987;82:121-126.
120. Francis JW, Todd RF, Boxer LA, et al. Histamine inhibits cell-spreading and C3bi receptor clustering and diminishes hydrogen peroxide production by adherent human neutrophils. *J Cell Physiol* 1991;147:128-137.
121. Uster PS, Pagano RE. Resonance energy transfer microscopy: observations of membrane-bound fluorescent probes in model membranes and in living cells. *J Cell Biol* 1986;103:1221-1234.
122. Zhou M-J, Poo H, Todd RF, et al. Surface-bound immune complexes trigger transmembrane proximity between complement receptor type 3 and the neutrophil's cortical microfilaments. *J Immunol* 1992;148:3550-3553.
123. Maher RJ, Cao D, Boxer LA, et al. Simultaneous calcium-dependent delivery of neutrophil lactoferrin and reactive oxygen metabolites to erythrocyte targets: evidence supporting granule-dependent triggering of superoxide release. *J Cell Physiol* 1993;156:226-234.
124. Kindzelskii AL, Zhou MJ, Haugland RP, et al. Oscillatory pericellular proteolysis and oxidant deposition during neutrophil locomotion. *Biophys J* 1998;74:90-97.
125. Garbett EA, Reed MWR, Brown NJ. Proteolysis in human breast and colorectal cancer. *Br J Cancer* 1999;81:287-293.
126. Kindzelskii AL, Yang Z, Nabel GJ, et al. Ebola virus secretory glycoprotein (sGP) disrupts FcgRIIIb to CR3 proximity on neutrophils. *J Immunol* 2000;165:953-958.
127. Li W, Yanoff M, Li Y, et al. Artificial senescence of bovine retinal pigment epithelial cells induced by near-ultraviolet in vitro. *Mech Age Devel* 1999;110:137-155.
128. Hed J. The extinction of fluorescence by crystal violet and its use to differentiate between attached and ingested microorganisms in phagocytosis. *FEMS Microbiol Lett* 1997;1:357-361.
129. LaBarca C, Paigen K. A simple, rapid, and sensitive DNA assay procedure. *Anal Biochem* 1980;102:344-352.
130. Hu CL, Crombie G, Franzblau C. A new assay for collagenolytic activity. *Anal Biochem* 1978;88:638-643.
131. Banda MJ, Werb Z. Mouse macrophage elastase: purification and characterization as a metalloproteinase. *Biochem J* 1981;1983:589-605.
132. Elner VM, Nielsen JC, Elner SG, et al. Immunophenotypic modulation of cultured human retinal pigment epithelial cells by gamma interferon and phytohemagglutinin-stimulated human T-lymphocytes (Abstract). *Invest Ophthalmol Vis Sci* 1989;30(Suppl):233.

133. Horino K, Kindezelskii AL, Elner VM, et al. Tumor cell invasion of model 3-dimensional matrices: demonstration of migratory pathways, collagen disruption, and intercellular cooperation. *FASEB J* 2001;15:932-939.
134. Esmaeli B, Elner VM, Elner SG, et al. Immunohistochemical detection of urokinase plasminogen activator receptor/Mo3 on human RPE cells (Abstract). *Invest Ophthalmol Vis Sci* 1994;35(Suppl):1759. Abstract 2334.
135. Vranka JA, Johnson E, Zhu Xianghong, et al. Discrete expression and distribution pattern of TIMP-3 in the human retina and choroid. *Curr Eye Res* 1997;15:102-110.
136. Lijnen HR, Arza B, Van Hoef B, et al. Inactivation of plasminogen activator inhibitor-1 by specific proteolysis with stromelysin-1 (MMP-3). *J Biol Chem* 2000;275:37645-37650.
137. Rizzolo LJ. Basement membrane stimulates the polarized distribution of integrins but not the Na,K-ATPase in the retinal pigment epithelium. *Cell Regul* 1991;2:939-949.
138. Simon DI, Wei Y, Zhang L, et al. Identification of urokinase receptor-integrin interaction site. Promiscous regulator of integrin function. *J Biol Chem* 2000;275:10228-10234.
139. Ross GD. Regulation of the adhesion versus cytotoxic functions of the Mac-1/CR3/alphaM beta2-integrin glycoprotein. *Crit Rev Immun* 2000;20:197-222.
140. May AE, Neumann FJ, Schomig A, et al. VLA-4 (alpha(4)beta(1)) engagement defines a novel activation pathway for beta(2) integrin-dependent leukocyte adhesion involving the urokinase receptor. *Blood* 2000;96:506-513.
141. Estreicher A, Muhlhauser J, Carpentier JL, et al. The receptor for urokinase-type plasminogen activator polarizes expression of the protease to the leading edge of migrating monocytes and promotes degradation of enzyme inhibitor complexes. *J Cell Biol* 1990;111:783-792.
142. Chu PG, Grunwald BG. Functional inhibition of retinal pigment epithelial cell-substrate adhesion with a monoclonal antibody against the beta I subunit of integrin. *Invest Ophthalmol Vis Sci* 1991;32:1763-1769.
143. Anderson DH, Guerin CJ, Matsumoto B, et al. Identification and localization of a beta-1 receptor from the integrin family in mammalian retinal pigment epithelial cells. *Invest Ophthalmol Vis Sci* 1990;31:81-93.
144. Lin W-L. Immunogold localization of extracellular matrix molecules in Bruch's membrane of the rat. *Curr Eye Res* 1989;8:1171-1178.
145. Moscatelli D, Jaffe E, Rifkin DB. Tetradecanoyl phorbol acetate stimulates latent collagenase production by cultured human endothelial cells. *Cell* 1980;20:343-351.
146. Kalebic T, Garbisa S, Glaser B, et al. Basement membrane collagen: degradation by migrating endothelial cells. *Science* 1983;221:281-283.
147. Li W, Yanoff M, Li Y, et al. Artificial senescence of bovine retinal pigment epithelial cels induced by near-ultraviolet in vitro. *Mech Age Devel* 1999;110:137-55.
148. Spencer WH. Macular diseases: pathogenesis: light microscopy. *Trans Am Acad Ophthalmol Otolaryngol* 1965;69:662-667.
149. Hogan MJ, Alvarado JA. Studies on the human macula, IV: aging changes in Bruch's membrane. *Arch Ophthalmol* 1967;77:410-420.
150. Garron LK. The ultrastructure of the retinal pigment epithelium, with observations on the choriocapillaris and Bruch's membrane. *Trans Am Ophthalmol Soc* 1963;61:545.
151. Green WR, Key SN. Senile macular degeneration: a histopathologic study. *Trans Am Ophthalmol Soc* 1977;75:180-254.
152. Green WR. Clinicopathologic studies of senile macular degeneration. In: Nicholson DH, ed. *Ocular Pathology Update*. New York: Masson Publishing Co; 1980:118.
153. Ishibashi T, Patterson R, Ohnishi Y, et al. Formation of drusen in the human eye. *Am J Ophthalmol* 1986;101:342-343.
154. Dhaliwal BS, Steinbrecher UP. Scavenger receptors and oxidized low density lipoproteins. *Clin Chim Acta* 1999;286:191-205.
155. Eeckhout Y, Vaes G. Further studies on the activation of procollagenase, the latent precursor of bone collagenase. Effects of lysosomal cathepsin B, plasmin and kallikrein, and spontaneous activation. *Biochem J* 1977;166:21-31.
156. Dingle JT. The secretion of enzymes into the pericellular environment. *Philosoph Trans R Soc London Series B*: *Biol Sci* 1975;271:315-332.
157. Davies P, Allison AC. The macrophage as a secretory cell in chronic inflammation. *Agents Actions* 1976;6:60-74.
158. Unanue ER. Secretory function of mononuclear phagocytes. *Am J Pathol* 1976;83:396-417.
159. Berman M, Leary R, Gage J. Collagenase from corneal cell cultures and its modulation by phagocytosis. *Invest Ophthalmol Vis Sci* 1979;18:588-601.
160. Harper E. Collagenases. *Annu Rev Biochem* 1980;49:1063-1078.
161. Salo T, Liotta LA, Tryggvason K. Purification and characterization of a murine basement membrane collagen-degrading enzyme secreted by metastatic tumor cells. *J Biol Chem* 1983;358:3058-3063.
162. Werb Z, Gordon S. Elastase secretion by stimulated macrophages: characterization and regulation. *J Exp Med* 1975;143:361-377.
163. Banda MJ, Clark EJ, Werb Z. Limited proteolysis by macrophage elastase inactivates human a-1-proteinase inhibitor. *J Exp Med* 1980;152:1563-1570.
164. Banda MJ, Clark EJ, Werb Z. Selective proteolysis of immunoglobulins by mouse macrophage elastase. *J Exp Med* 1983157:1184-1196.
165. Penfild PL, Provis JM, Billson FA. Age-related macular degeneration: ultrastructural studies of the relationship of leukocytes to angiogenesis. *Graefes Arch Clin Exp Ophthalmol* 1987;225:70-76.
166. Penfild PL, Killingsworth MS, Sarks SH. Senile macular degeneration: the involvement of immunocomponent cells. *Graefes Arch Clin Exp Ophthalmol* 1987;223:69-76.
167. Loeffler KU, Lee R. Basal linear deposit in the human macula. *Graefes Arch Clin Exp Ophthalmol* 1986;224:493-501.
168. Sunderkotter C, Steinbrink K, Goebeler M, et al. Macrophages and angiogenesis. *J Leuk Biol* 1994;55:410-422.
169. Polverini PJ, Cotran PS, Gimbrone MA Jr, et al. Activated macrophages induce vascular proliferation. *Nature* 1977;269:804-806.
170. Anin R, Puklin JE, Frank RN. Growth factor localization in choroidal neovascular membranes of age-related macular degeneration. *Invest Ophthalmol Vis Sci* 1994;35:3178-3188.
171. Lopez PF, Sippy BD, Lambert HM, et al. Transdifferentiated retinal pigment epithelial cells are immunoreactive for vascular endothelial growth factor in surgically excised age-related macular degeneration neovascular membranes. *Invest Ophthalmol Vis Sci* 1996;37:855-868.
172. Oh H, Takagi H, Takagi C, et al. The potential angiogenic role of macrophages in the formation of choroidal neovascular membranes. *Invest Ophthalmol Vis Sci* 1999;40:1891-1898.
173. Otani A, Takagi H, Oh H, et al. Expression of angiopoietins and Tie2 in human choroidal neovascular membranes. *Invest Ophthalmol Vis Sci* 1999;40:1912-1920.
174. Bian ZM, Elner SG, Streiter RM, et al. IL-4 potentiates IL-1β and TNF-α stimulated IL-8 and MCP-1 protein production in human retinal pigment epithelial cells. *Curr Eye Res* 1999;18:349-357.

175. Elner VM, Streiter RM, Elner SG, et al. Neutrophil chemotactic factor (IL-8) gene expression by cytokine-treated retinal pigment epithelial cells. *Am J Pathol* 1990;136:745-750.
176. Pepper MS, Montesano R, Mandriota SJ, et al. Angiogenesis: a paradigm for extracellular proteolysis during cell migration and morphogenesis. *Enzyme Prot* 1996;49:138-162.
177. Davis GE, Pintar Allen KA, Salazar R, et al. Matrix metalloproteinase-1 and -9 activation by plasmin regulates a novel endothelial cell-mediated mechanism of collagen gel contraction and capillary tube regression in three-dimensional collagen matrices. *J Cell Sci* 2001;114:917-930.
178. DeNichilo MO, Burns GF. Granulocyte-macrophage and macrophage colony-stimulating factors diffentially regulate alpha v integrin expression on cultured human macrophages. *PNAS* 1993;90:2517-2521.
179. Brooks PC, Stromblad S, Sanders LC, et al. Localization of matrix metalloproteinase MMP-2 to the surface of invasive cells by interaction with integrin alpha v beta 3. *Cell* 1996;85:683-685.
180. Gailit J, Welch MP, Clark RA. TGF-beta a stimulates expression of keratinocyte integrins during re-epithelialization of cutaneous wounds. *J Invest Dermatol* 1994;103:221-227.
181. Brown SL, Lundgren CH, Nordt T, et al. Stimulation of migration of human aortic smooth muscle cells by vitronectin: implications for atherosclerosis. *Cardiovasc Res* 28:1815-1820.
182. Marshall JF, Nesbitt SA, Helfrich MH, et al. Integrin expression in human melanoma cell lines: heterogeneity of vitronectin receptor composition and function. *Int J Cancer* 1991;49:9224-9231.
183. Khatib AM, Nip J, Fallavollita L, et al. Regulation of urokinase plasminogen activator/plasmin-mediated invasion of melanoma cells by the integrin vitronectin receptor. *Int J Cancer* 2001;91:300-308.
184. Kanse SM, Kost C, Wilhelm OG, et al. The urokinase receptor is a major vitronectin-binding protein on endothelial cells. *Exp Cell Res* 1996;224:344-353.
185. Montgomery AM, Reisfeld RA, Cheresh DA. Integrin alpha v beta 3 rescues melanoma cells from apoptosis in three-dimensional dermal collagen. *Proc Natl Acad Sci USA* 1994;91:8856-8860.
186. Seftor RE, Seftor EA, Gehlsen KR, et al. Role of the alpha v beta 3 integrin in human melanoma cell invasion. *Proc Natl Acad Sci USA* 1992;89:1557-1561.
187. Stahl A, Mueller BM. Melanoma cell migration on vitronectin: regulation by components of the plasminogen activation system. *Int J Cancer* 1997;71:116-122.
188. Wei Y, Waltz DA, Rao N, et al. Identification of the urokinase receptor as an adhesion receptor for vitronectin. *J Biol Chem* 1994;269:32380-32388.
189. Montgomery AMP, De Clerck YA., Langley KE, et al. Melanoma-mediated dissolution of extracellular matrix: contribution of urokinase-dependent and metalloproteinase-dependent proteolytic pathway. *Cancer Res* 1993;53:693-700.
190. Monsky WL, Lin CY, Aoyama A, et al. A potential marker protease of invasiveness, seprase, is localized on invadopodia of human malignant melanoma cells. *Cancer Res* 1994;54:5702-5710.
191. McCawley L J, Matrisian LM. Matrix metalloproteinases: multifunctional contributors to tumor progression. *Mol Med Today* 2000;4:149-156.
192. Curran S, Murray GI. Matrix metalloproteinases in tumor invasion and metastasis. *J Pathol* 1999;189:300-308.
193. Ellerbrock SM, Stack MS. Membrane associated matrix metalloproteinases in metastasis. *Bioessays* 1999;21:940-949.
194. Murphy G, Gavrilovic J. Proteolysis and cell migration: creating a path? *Curr Opin Cell Biol* 1999;11:614-621.
195. Dano K, Romer J, Nielsen BS, et al. Cancer invasion and tissue remodeling: cooperation of protease systems and cell types. *APMIS* 1999;107:120-127.
196. Reich R, Thompson EW, Iwamoto Y, et al. Effects of inhibitors of plasminogen activator, serine proteinases, and collagenases IV on the invasion of basement membranes by metastatic cells. *Cancer* Res 1988;48:3307-3312.
197. Hart IR, Fidler IJ. An in vitro quantitative assay for tumor cell invasion. *Cancer Res* 1978;38:3218-3224.
198. Poste G, Doll J, Hart IR, et al. In vitro selection of murine B 16 melanoma variants with enhanced tissue-invasive properties. *Cancer Res* 1980;40:1636-1644.
199. Towle MJ, Lee A, Maduakor EC, et al. Inhibition by 4-substituted benzo [b] thiophene-2-carboxamidines: an important new class of selective synthetic urokinase inhibitor. *Cancer Res* 1993;53:2553-2559.
200. Sitrin RG, Todd RF III, Albrecht E, et al. The urokinase receptor (CD87) facilities CD11b/CD18-mediated adhesion of human monocytes. *J Clin Invest* 1996;97:1942-1951.
201. Gyteko M, Todd III R, Wilkinson C, et al. The urokinase receptor is required for monocyte chemotaxis in vitro. *J Clin Invest* 1994;93:1380-1387.
202. Koshelnick Y, Ehart M, Stockinger H, et al. Mechanisms of signaling through urokinase receptor and the cellular response. *Thromb Haemostasis* 1999;82:305-311.
203. Sitrin R, Pan P, Harper H, et al. Urokinase receptor (CD87) aggregation triggers phosphoinositide hydrolysis and intracellular calcium mobilization in mononuclear phagocytes. *J Immunol* 1999;163:6193-6200.
204. Blasi F. Urokinase and urokinase receptor: a paracrine/autocrine system for regulating cell migration and invasiveness. *Bioessays* 1993;5:105-111.